DIPARTIMENTO DI INGEGNERIA ELETTRICA E DELL'INFORMAZIONE

VERNIER-EFFECT STRATEGIES FOR EFFICIENT INTEGRATED OPTICAL SENSING

Prof. Vittorio M. N. Passaro

Photonics Research Group, Dipartimento di Ingegneria Elettrica e dell'Informazione

Politecnico di Bari, Via E. Orabona n. 4, 70125 Bari - Italy

vittorio.passaro@poliba.it, WEB page: http://dee.poliba.it/photonicsgroup

Keynote speech

SENSORSDEVICES 2018, Venice, 17th September, 2018

PHOTONICS RESEARCH GROUP

OUTLINE

- **PHOTONIC SENSING APPLICATIONS**

- **PHOTONIC DEVICES FOR SENSING APPLICATIONS**
  - Design of photonic waveguides;
  - Optical sensing principles;
  - Group IV material systems and alloys.

- **PHOTONIC ARCHITECTURES BASED ON VERNIER EFFECT**
  - The Vernier effect for photonic sensing;
  - Vernier sensors based on cascaded microring resonators;
  - Vernier sensors based on cascaded ring resonator and MZI;
  - Vernier sensors based on cascaded ring resonator and MZI with a Sagnac loop.

- **ADVANCED PHOTONIC SENSORS OPERATING IN THE NEAR-IR AND MID-IR**
  - Sensing principles for gas detection in the mid-IR;
  - Photonic sensors based on the Vernier effect for methane and ethane detection;
  - Experimental demonstration of the Vernier effect in integrated Photonics.

- **CONCLUSIONS**

OUTLINE

- **PHOTONIC SENSING APPLICATIONS**

- **PHOTONIC DEVICES FOR SENSING APPLICATIONS**
  - Design of photonic waveguides;
  - Optical sensing principles;
  - Group IV material systems and alloys.

- **PHOTONIC ARCHITECTURES BASED ON VERNIER EFFECT**
  - The Vernier effect for photonic sensing;
  - Vernier sensors based on cascaded microring resonators;
  - Vernier sensors based on cascaded ring resonator and MZI;
  - Vernier sensors based on cascaded ring resonator and MZI with a Sagnac loop.

- **ADVANCED PHOTONIC SENSORS OPERATING IN THE NEAR-IR AND MID-IR**
  - Sensing principles for gas detection in the mid-IR;
  - Photonic sensors based on the Vernier effect for methane and ethane detection;
  - Experimental demonstration of the Vernier effect in integrated Photonics.

- **CONCLUSIONS**

PHOTONIC SENSING APPLICATIONS

PHOTONIC SENSORS FOR BIOMEDICAL APPLICATIONS:

- Monitoring of protein aggregation processes (e.g., biotin-streptavidin, biotin-avidin, antibody-antigen);
- Real-time monitoring of DNA hybridization;
- *In vitro-in vivo* detection of viruses, bacteria, tumor and cancer biomarkers;
- Monitoring of glucose in blood, pH, biological temperature.

PHOTONIC SENSORS FOR SAFETY AND FOOD QUALITY CONTROL:

- Explosive-trace detection (TNT, RDX);
- Measure of angular velocity in gyroscopes (automotive, aerospace);
- Detection of pathogenic microorganisms (bacteria, viruses).

PHOTONIC SENSORS FOR ENVIRONMENTAL MONITORING:

- Detection of harmful gases (CO_2, CH_4, CO, NO, SO_2);
- Monitoring of electromagnetic fields;
- Detection of pollutants in liquids (e.g., pesticides, heavy metals).

Photonic sensing applications

Photonic integrated sensing: (label-free) applications

- Monitoring of protein aggregation processes (e.g., biotin-streptavidin, biotin-avidin, antibody-antigen);
- Real-time monitoring of DNA hybridization;
- *In vitro-in vivo* detection of viruses, bacteria, tumor and cancer biomarkers;
- Monitoring of glucose in blood, pH, biological temperature;
- Explosive-trace detection (TNT, RDX);
- Detection of pathogenic microorganisms;
- Detection of harmful gases (e.g., CO_2, CH_4, CO, NO, SO_2);
- Detection of pollutants in liquids (e.g., pesticides, heavy metals).

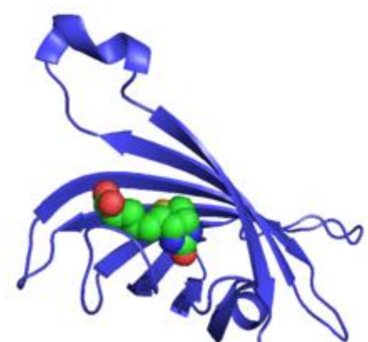

PHOTONICS RESEARCH GROUP

OUTLINE

- PHOTONIC SENSING APPLICATIONS

- PHOTONIC DEVICES FOR SENSING APPLICATIONS
  - Design of photonic waveguides;
  - Optical sensing principles;
  - Group IV material systems and alloys.

- PHOTONIC ARCHITECTURES BASED ON VERNIER EFFECT
  - The Vernier effect for photonic sensing;
  - Vernier sensors based on cascaded microring resonators;
  - Vernier sensors based on cascaded ring resonator and MZI;
  - Vernier sensors based on cascaded ring resonator and MZI with a Sagnac loop.

- ADVANCED PHOTONIC SENSORS OPERATING IN THE NEAR-IR AND MID-IR
  - Sensing principles for gas detection in the mid-IR;
  - Photonic sensors based on the Vernier effect for methane and ethane detection;
  - Experimental demonstration of the Vernier effect in integrated Photonics.

- CONCLUSIONS

SUB-MICROMETER OPTICAL WAVEGUIDES IN SOI TECHNOLOGY

SILICON-WIRE WAVEGUIDE

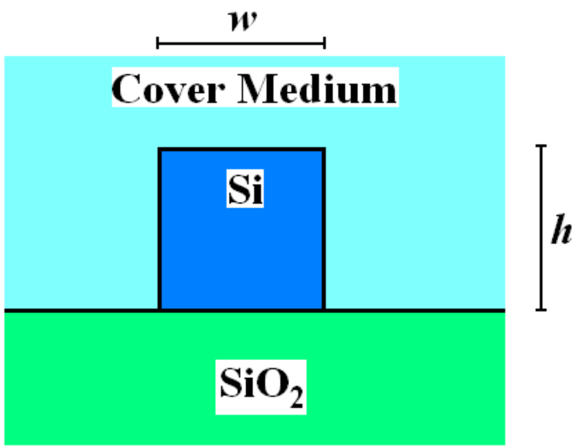

RIB WAVEGUIDE

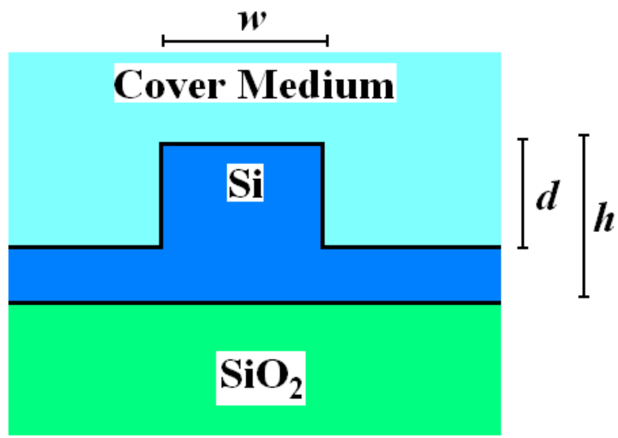

SLOT WAVEGUIDE

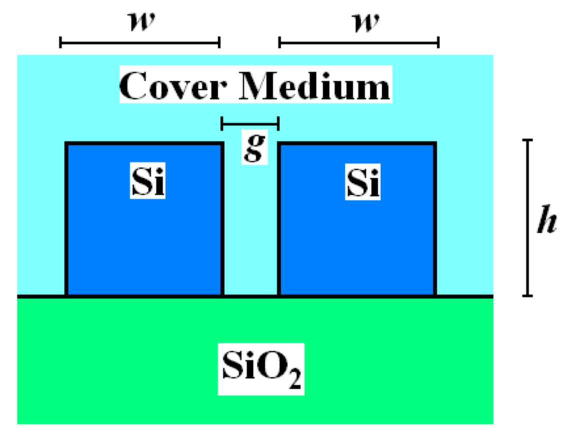

$$\left|\mathbf{E}(x,y)\right|^2$$

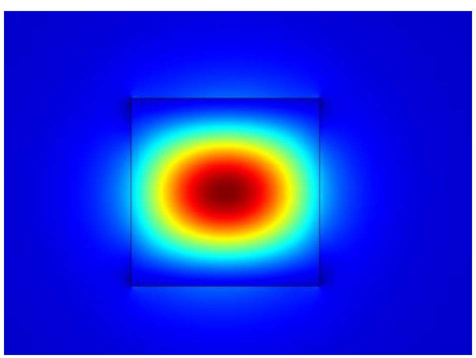

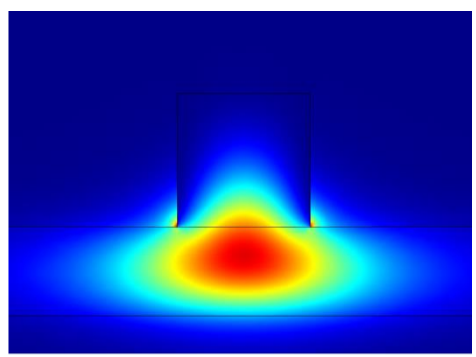

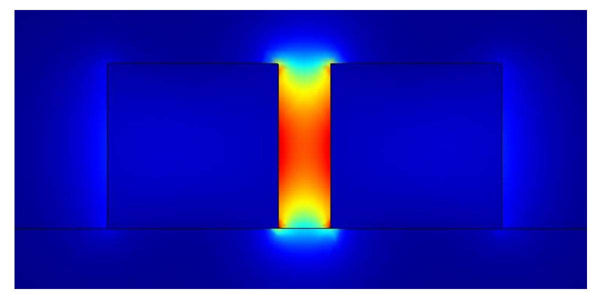

Finite element method (FEM) simulations

SILICON-ON-INSULATOR PHOTONIC WAVEGUIDES FOR SENSING APPLICATIONS

SILICON-WIRE WAVEGUIDE

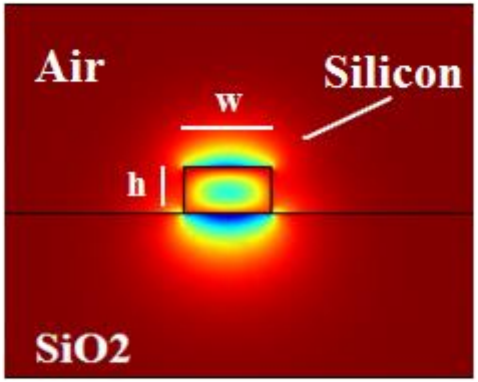

h = 250nm, w = 450nm, λ = 1.55μm, quasi-TM.

MEMBRANE WAVEGUIDE

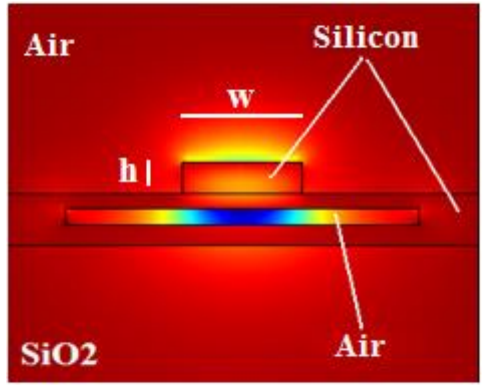

h = 250nm, w = 800nm, λ = 1.55μm, quasi-TM.

SLOT WAVEGUIDE

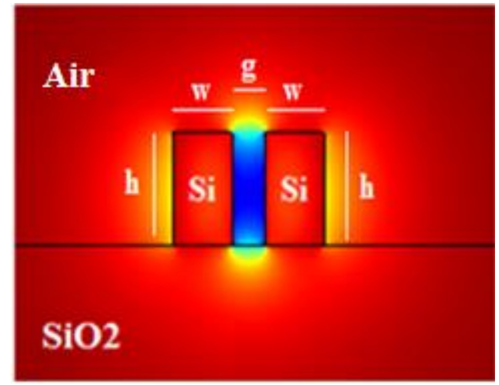

h = 324nm, w = 180nm, g = 100nm, λ = 1.55μm, quasi-TE.

Finite element method (FEM) simulations

- ✓ **SILICON-ON-INSULATOR (SOI) TECHNOLOGY**
  - STANDARD TECHNOLOGICAL PLATFORM (E.G. MICROELECTRONICS).
- ✓ **EVANESCENT FIELD PHOTONIC BIOSENSING**
  - HIGH REFRACTIVE INDEX CONTRAST (Δn ≈ 2);
  - HIGH OPTICAL FIELD CONFINEMENT;
  - SUB-MICROMETER PHOTONIC DEVICE DIMENSIONS
  - LOW LOSSES (< 1 dB/cm).

Slot waveguides →

$$\left|\frac{E_L}{E_H}\right| = \left(\frac{n_H}{n_L}\right)^2$$

Electric field discontinuity

PHOTONICS RESEARCH GROUP

PHOTONIC SENSING PRINCIPLES

HOMOGENEOUS SENSING

Applications

IR cover	*IR Gas/Liquid*	Δn_c
$n_{air} = 1$	$n_{He} = 1.000035$	0.0035
$n_{air} = 1$	$n_{CO2} = 1.000059$	0.0059
$n_{air} = 1$	$n_{Ar} = 1.000278$	0.0278
$n_{air} = 1$	$n_{N2} = 1.000294$	0.0294
$n_{air} = 1$	$n_{C2H2} = 1.000593$	0.0593
$n_{water} = 1.33$	$n_{NaCl} \approx 1.33$	0.0018

Refractive indices @ 1.55µm

$$S_h = \frac{\partial n_{eff}}{\partial n_c}$$

SURFACE SENSING

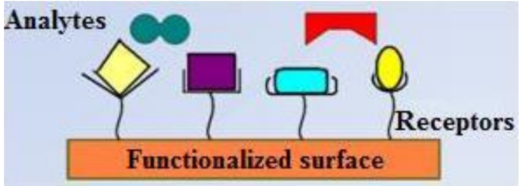

ρ ≈ 2÷10 nm

$$S_s = \frac{\partial n_{eff}}{\partial \rho}$$

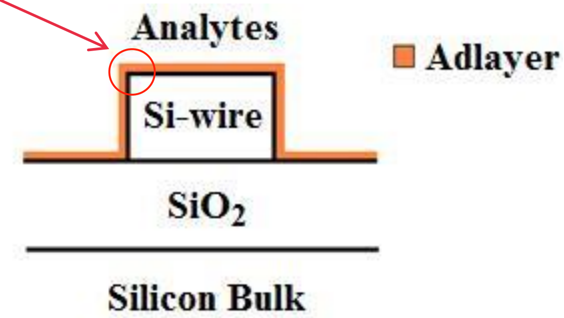

OPTICAL ABSORPTION

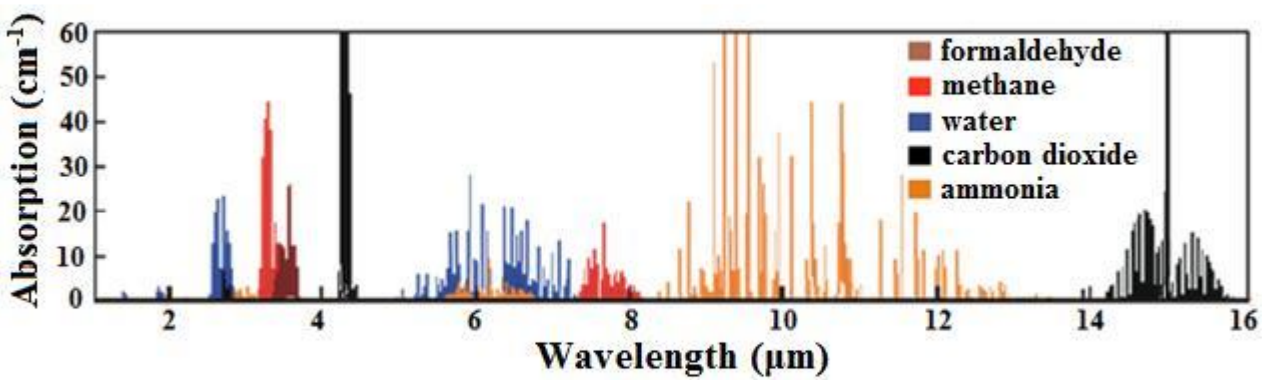

Absorption spectra of gases and liquid solutions in the mid-IR

Beer-Lambert law

$$I = I_0 \exp(-\alpha L); \quad \alpha = \varepsilon C$$

C = analyte concentration

ε = molar absorption coefficient

PHOTONICS RESEARCH GROUP

Group IV material systems and alloys

Slot waveguides optimized for homogeneous sensing @ λ = 3.39 µm e λ = 2.883 µm

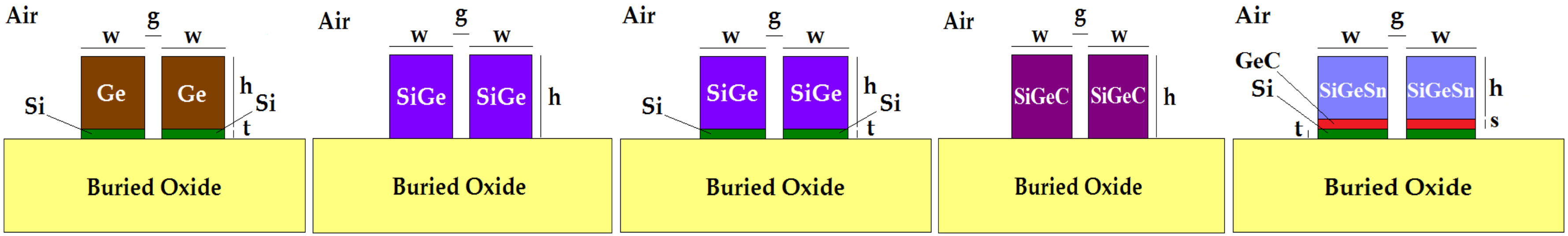

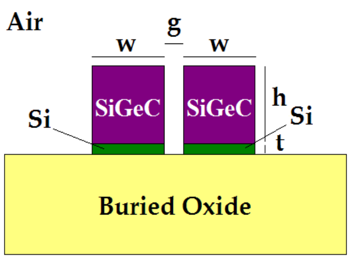

Complex fabrication but ultra-high performance!

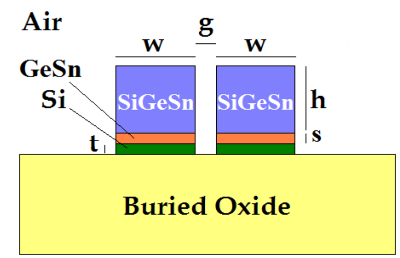

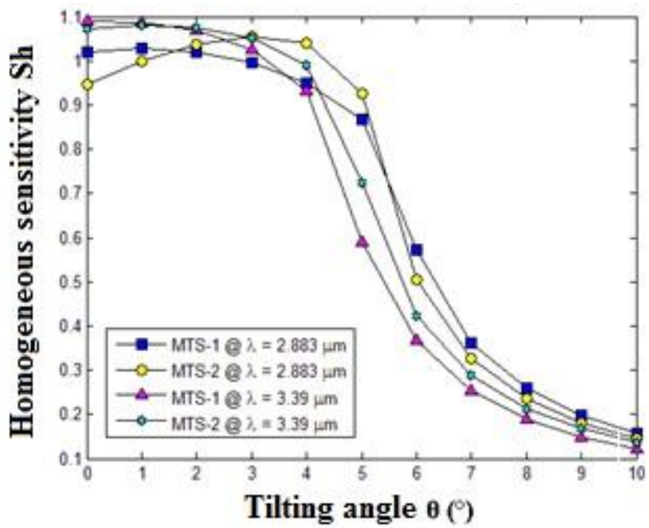

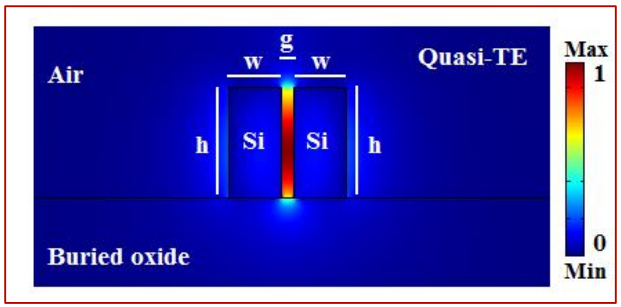

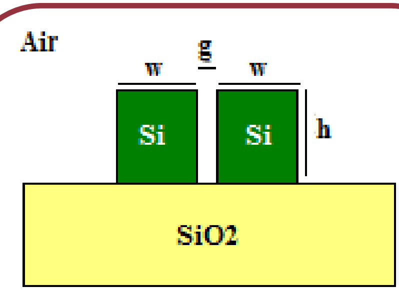

h = 950nm, w = 460nm, g = 100nm, λ = 3.39µm.
S_h = 1.01, Γ_c = 0.6, Γ_s = 0.788

MTS-1: Ge(0.78)Si(0.08)Sn(0.14)/Ge(0.97)C(0.03)/Si – ***t*** = 20 nm, ***w*** = 390 nm, ***s*** = 50 nm, ***h*** = 560 nm.
MTS-2: Ge(0.78)Si(0.08)Sn(0.14)/Ge(0.91)Sn(0.09)/Si – ***t*** = 20 nm, ***w*** = 380 nm, ***s*** = 50 nm, ***h*** = 520 nm.

PHOTONICS RESEARCH GROUP

OVERVIEW OF SOI SENSOR PERFORMANCE AND ARCHITECTURES

Architecture	Technology	Performance	Size	Analyte
MZI	SOI	8.7×10^{-7} RIU/ppm	2.1mm-long	BTEX
MZI	CMOS-compatible	0.3 pg/mm^2	1.8mm-long (×9 - array)	IgG goat ,rabbit
SPR	CMOS-compatible	3022nm/RIU 70pg/mm^2	~ 800µm^2	Molecules
Grating	SOI	~ 120nm ~ 10^{-4}RIU	173µm-long	Biological reactions
PhC-slot	SOI	100ppm	300µm-long	Methane
PhC-slot	SOI	510nm/RIU 1×10^{-5}RIU	2µm-cavity length	Gases N_2, He, CO_2
Directional coupler	SOI	0.1 g/L	~ 1mm^2 (footprint)	Glucose
MMI	SOI	+152, -172	1.607µm-long	Glucose, etanole
Slot-ring resonator	SOI	2000nm/RIU 3.8×10^{-5}RIU	~ 1mm^2 (footprint)	Molecules, Gases
Ring resonator	SOI	60fM	175×500µm^2 (×32- array)	DNA
Cascaded resonators	SOI	2169nm/RIU 8.3×10^{-6}RIU	200×70µm^2 (2x- array)	NaCl, molecules

Some examples in SOI technology platform:

- Mach-Zehnder Interferometers (MZI)
- Directional Couplers
- Photonic Crystals (PhC)
- Surface Plasmon Resonance (SPR)
- Integrated Bragg Gratings
- Multi-Mode Interferometers (MMI)
- Ring Resonators
- Cascade-coupled Ring Resonators
- Integrated Waveguides

OUTLINE

- **Photonic sensing applications**

- **Photonic devices for sensing applications**
  - Design of photonic waveguides;
  - Optical sensing principles;
  - Group IV material systems and alloys.

- **Photonic architectures based on Vernier effect**
  - The Vernier effect for photonic sensing;
  - Vernier sensors based on cascaded microring resonators;
  - Vernier sensors based on cascaded ring resonator and MZI;
  - Vernier sensors based on cascaded ring resonator and MZI with a Sagnac loop.

- **Advanced photonic sensors operating in the near-IR and mid-IR**
  - Sensing principles for gas detection in the mid-IR;
  - Photonic sensors based on the Vernier effect for methane and ethane detection;
  - Experimental demonstration of the Vernier effect in integrated Photonics.

- **Conclusions**

THE VERNIER EFFECT FOR PHOTONIC SENSING

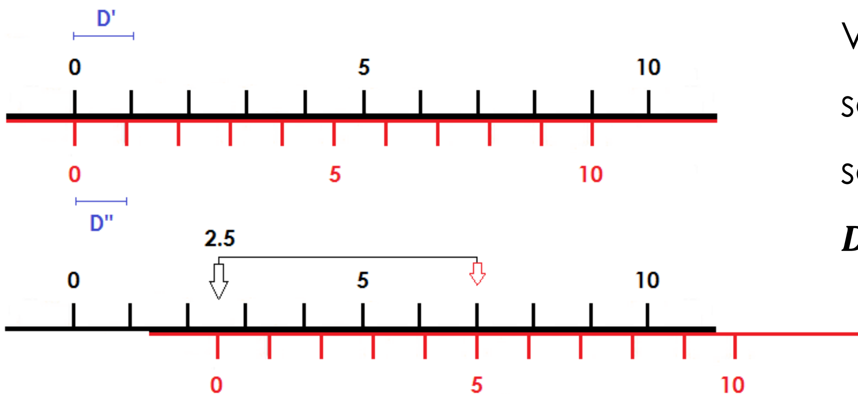

Vernier effect achieved by using two frequency scales with different periods D' and D'', where one scale slides along the other scale which is fixed.

$D'' = D' \cdot [(n-1)/n]$ with n a positive integer number.

$$\frac{FSR''}{FSR'} = \frac{L'}{L''} = \frac{n-1}{n}$$

THE VERNIER EFFECT IN PHOTONIC INTEGRATED CIRCUITS

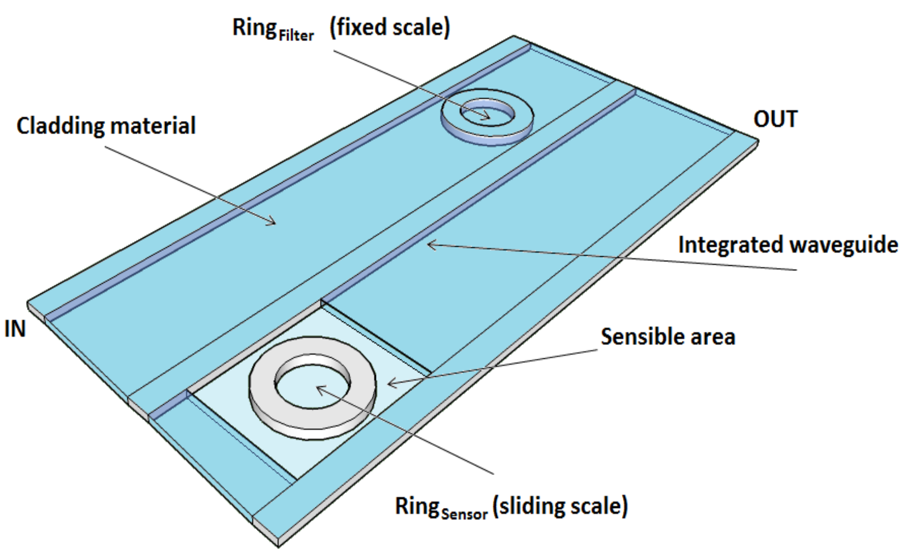

Schematic of a Vernier architecture based on cascaded integrated ring resonators optimized for sensing purposes

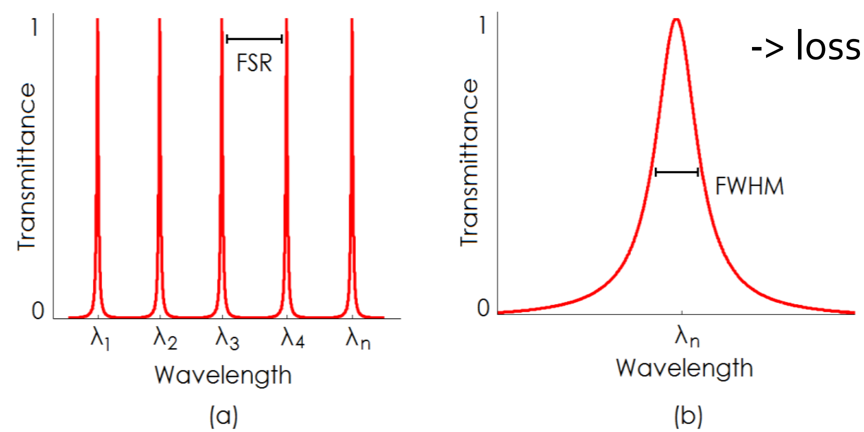

(a) Qualitative planar ring resonator spectrum; (b) zoom in a resonant peak at the wavelength λ_n

PHOTONICS RESEARCH GROUP

VERNIER SENSORS BASED ON CASCADED MICRORING RESONATORS

Vernier transmittance: $T_v = T_{Ring\#1} \cdot T_{Ring\#2} = T_{Filter} \cdot T_{Sensor}(n_{cover})$;

$$FSR = \frac{c}{L \cdot n_{eff}}$$

- The first regime (optical filtering): $\Delta FSR > \min(\Delta\lambda_{FWHM(Ring\#1,Ring\#2)})$;
- The second regime (**optical sensing**): $\Delta FSR < \min(\Delta\lambda_{FWHM(Ring\#1,Ring\#2)})$.

First regime

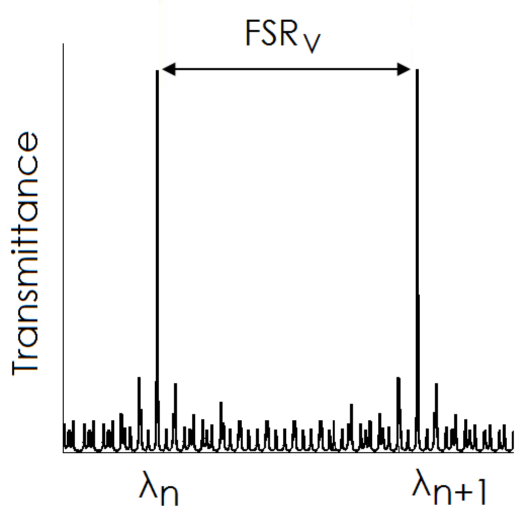

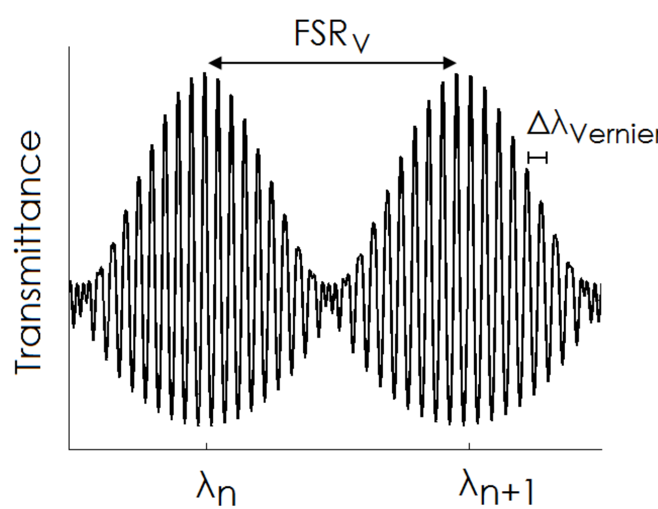

Second regime

Similar lengths (and large n)

Sensing performance can be enhanced with respect to a single ring resonator:

Vernier gain: $G_v = \frac{FSR_{filter}}{|\Delta FSR|}$;

Wavelength shift induced by sensing: $\Delta\lambda_v = \Delta\lambda_{res} \cdot G_v$;

Wavelength sensitivity: $S_{\lambda,v} = S_\lambda \cdot G_v$;

Overall Free Spectral Range: $FSR_v = \frac{FSR_{filter} \cdot FSR_{sensor}}{|\Delta FSR|}$;

Homogeneous sensing refractive index variations:

$\Delta n_{c,min} = n_g^0 \frac{\Delta FSR}{\lambda_{res}} S_h^{-1}$; $\Delta n_{c,max} = \frac{FSR_v}{S_{\lambda,v}}$;

Surface sensing refractive index variations:

$\Delta t_{ad,min} = n_g^0 \frac{\Delta FSR}{\lambda_{res}} S_S^{-1}$; $\Delta t_{ad,max} = \frac{FSR_v}{S_{\lambda,v}}$.

PHOTONICS RESEARCH GROUP

MODELING OF ADVANCED PHOTONIC ARCHITECTURES BASED ON RESONANT MICROCAVITIES

Generalized approach

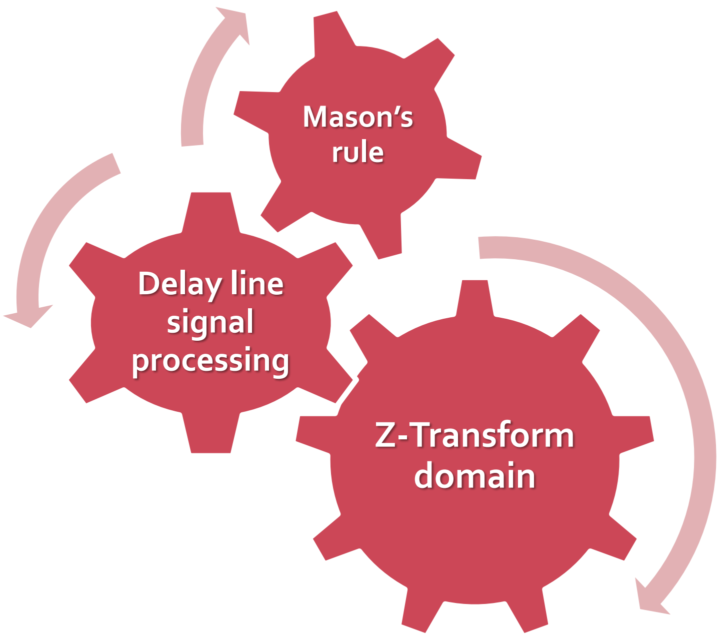

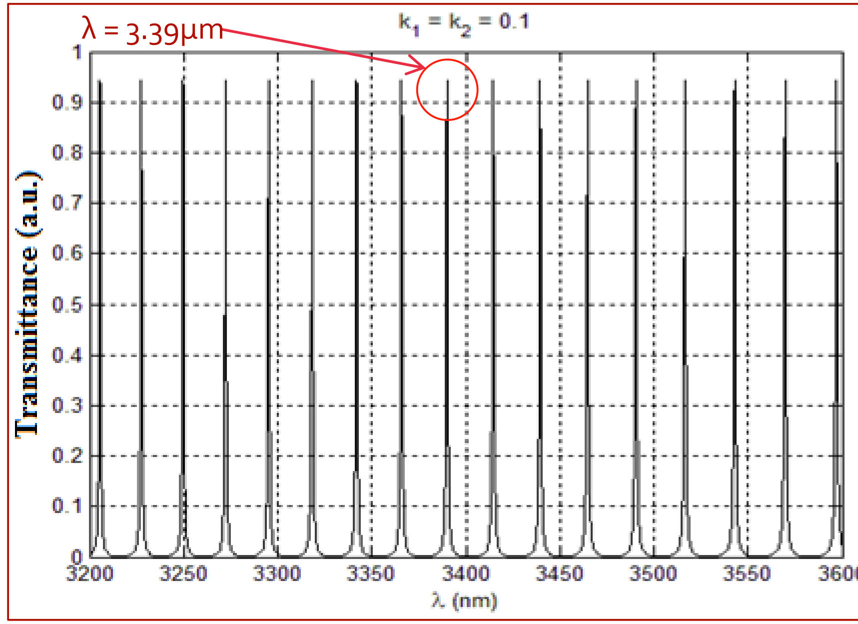

Plot

Resonant microcavity

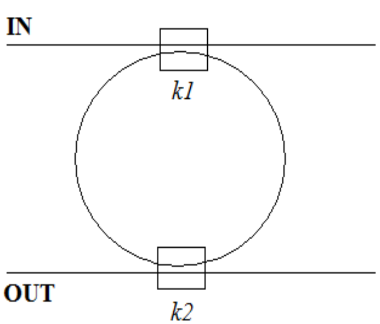

Loss-free directional couplers
(q1 = q2 = 0)

SFG

Signal Flow Graph

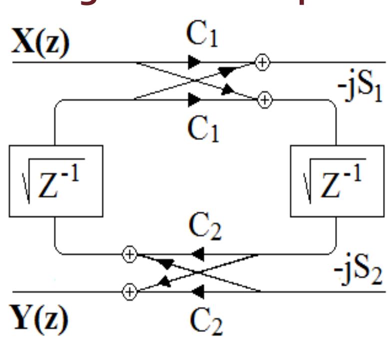

$$S_i = \sqrt{k_i};\ C_i = \sqrt{1-k_i}$$

Math

Transmittance

$$T_f(z) = \frac{Y(z)}{X(z)} = \frac{q_1 q_2 S_1 S_2 \sqrt{\gamma_1 z^{-1}}}{1 - q_1 q_2 C_1 C_2 \gamma_1 z^{-1}}$$

$$\gamma = \exp(-\alpha \cdot L)$$
$$z = \exp(-j 2\pi T \nu)$$

$$T = \frac{L \cdot n_{eff}}{c} \Rightarrow FSR = \frac{1}{T} = \frac{c}{L \cdot n_{eff}}$$

PHOTONICS RESEARCH GROUP

MODELING OF ADVANCED PHOTONIC ARCHITECTURES BASED ON CASCADED RESONANT MICROCAVITIES FOR THE VERNIER EFFECT

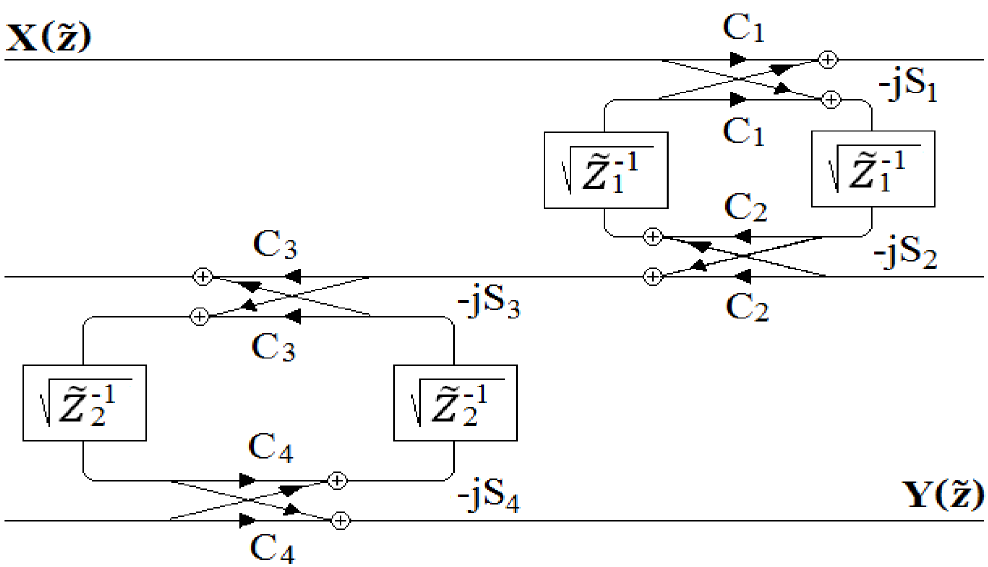

Signal Flow Graph of a Vernier architecture based on cascade-coupled racetrack resonators.

$$T_v(\tilde{z}) = \frac{S_1 S_2 S_3 S_4 \sqrt{\gamma_1 \gamma_2 \tilde{z}_1^{-1} \tilde{z}_2^{-1}}}{1 - C_1 C_2 \gamma_1 \tilde{z}_1^{-1} - C_3 C_4 \gamma_2 \tilde{z}_2^{-1} + C_1 C_2 C_3 C_4 \gamma_1 \gamma_2 \tilde{z}_1^{-1} \tilde{z}_2^{-1}}$$

Mason's rule direct formulation.

$$T_v(\tilde{z}) = \frac{S_1 S_2 \sqrt{\gamma_1 \tilde{z}_1^{-1}}}{1 - C_1 C_2 \gamma_1 \tilde{z}_1^{-1}} \times \frac{S_3 S_4 \sqrt{\gamma_2 \tilde{z}_2^{-1}}}{1 - C_3 C_4 \gamma_2 \tilde{z}_2^{-1}}$$

Mason's rule formulation applied to the product of the two cascade-coupled racetrack resonators.

PHOTONICS RESEARCH GROUP

Photonic sensors based on the Vernier effect

Transmittance of the photonic sensor based on the Vernier effect

$$T_{tot}(z) = T_{filter} \cdot T_{sensor}(n_c)$$

⇩

$$T_{tot}(z) = \frac{\sqrt{k_1 k_2 k_3 k_4}\sqrt{\gamma_1 \gamma_2 z_{tot}}}{1 - \gamma_1 z_1 \sqrt{(1-k_1)(1-k_2)} - \gamma_2 z_2 \sqrt{(1-k_3)(1-k_4)} + \gamma_1 \gamma_2 z_{tot} \sqrt{(1-k_1)(1-k_2)(1-k_3)(1-k_4)}}$$

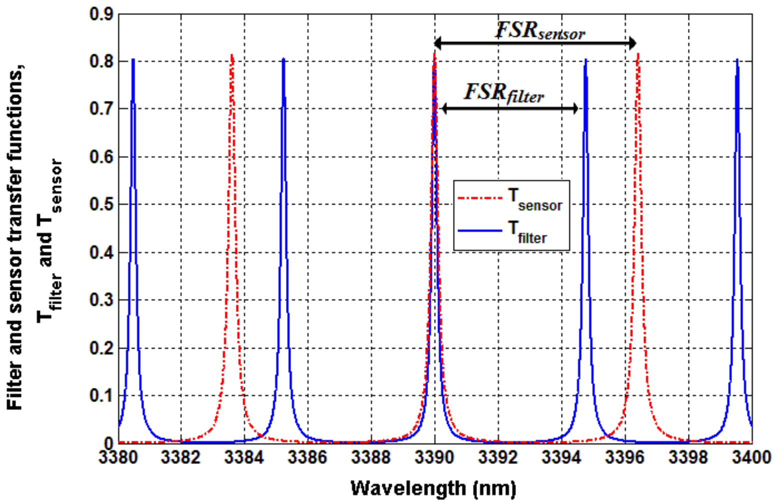

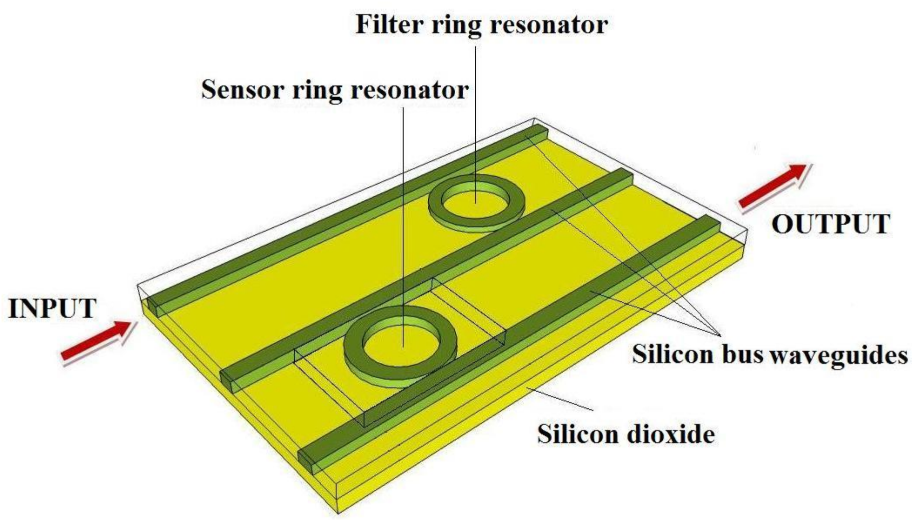

INTERNAL VIEW

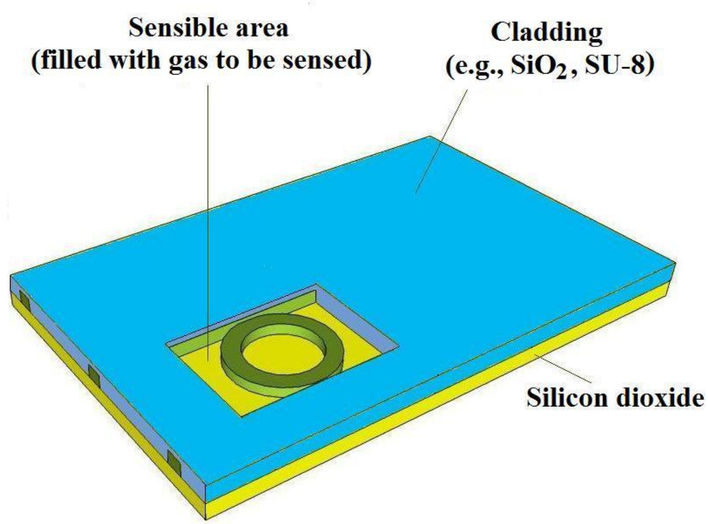

EXTERNAL VIEW

Photonic sensor based on the Vernier effect

PHOTONICS RESEARCH GROUP

PHOTONIC SENSORS BASED ON THE VERNIER EFFECT

OPERATIVE REGIMES

FIRST OPERATIVE REGIME	SECOND OPERATIVE REGIME

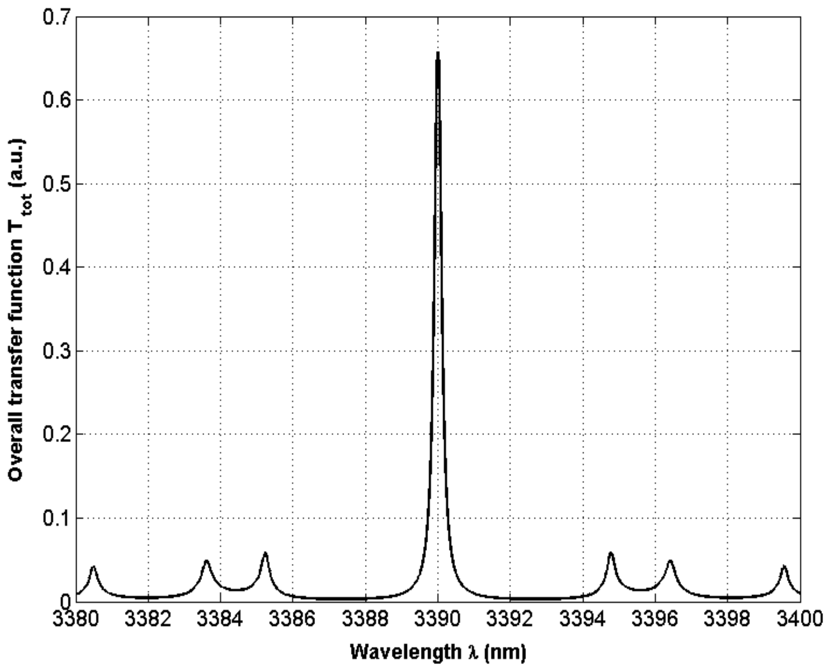

$$\Delta FSR > \Delta\lambda_{FWHM\,(filter,sensor)}$$

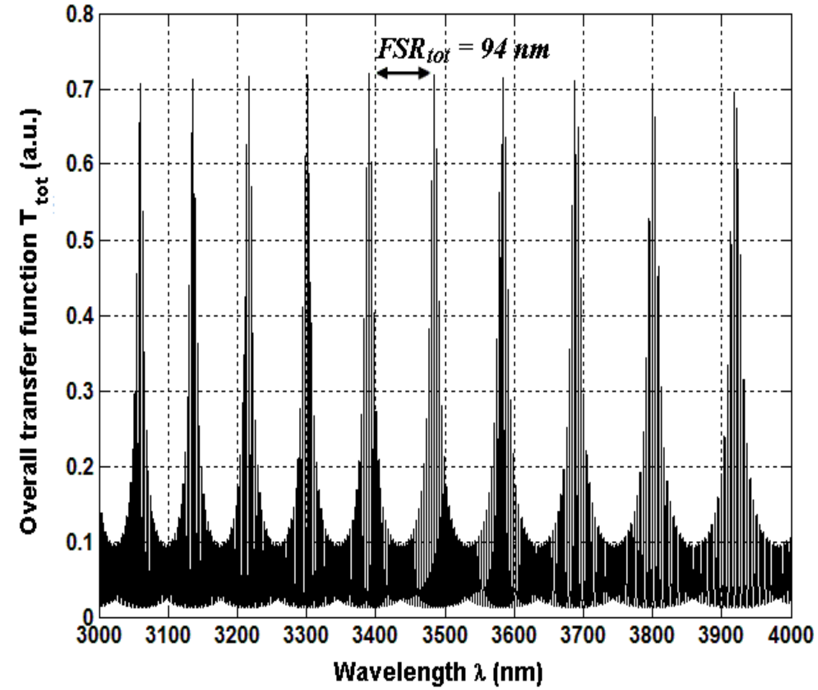

$$\Delta FSR < \Delta\lambda_{FWHM\,(filter,sensor)}$$

[second regime]

GAIN FACTOR

$$G = FSR_{filter} / \Delta FSR$$

Single ring resonator

$$\Delta\lambda_{sensor} = \lambda_{sensor} \cdot \left(\Delta n_{eff} / \Delta n_c\right)$$

$$S_{\lambda} = \Delta\lambda / \Delta n_c = \left(\Delta\lambda_{sensor} / \Delta n_{eff}\right) \cdot \left(\Delta n_{eff} / \Delta n_c\right)$$

Cascaded ring resonators

$$\Delta\lambda_{tot} = \Delta\lambda_{sensor} \cdot G$$

$$S_{\lambda,tot} = \Delta\lambda_{tot} / \Delta n_c = S_{\lambda} \cdot G$$

OUTLINE

- PHOTONIC SENSING APPLICATIONS

- PHOTONIC DEVICES FOR SENSING APPLICATIONS
  - Design of photonic waveguides;
  - Optical sensing principles;
  - Group IV material systems and alloys.

- PHOTONIC ARCHITECTURES BASED ON VERNIER EFFECT
  - The Vernier effect for photonic sensing;
  - Vernier sensors based on cascaded microring resonators;
  - Vernier sensors based on cascaded ring resonator and MZI;
  - Vernier sensors based on cascaded ring resonator and MZI with a Sagnac loop.

- ADVANCED PHOTONIC SENSORS OPERATING IN THE NEAR-IR AND MID-IR
  - Sensing principles for gas detection in the mid-IR;
  - Photonic sensors based on the Vernier effect for methane and ethane detection;
  - Experimental demonstration of the Vernier effect in integrated Photonics.

- CONCLUSIONS

VERNIER SENSORS BASED ON CASCADED RING RESONATOR AND MZI

Working Principle & Transfer Function

Working principle

$$\overline{E}_i = \overline{e}_0(x,y)e^{-j\beta z}e^{-j\phi} \quad ; \quad i=(1,2)$$

$$\overline{E}_{out} = 2\overline{e}_0(x,y)e^{-j\beta z}e^{-j\frac{\Delta\phi}{2}}\cos(\Delta\phi/2)$$

$$\Delta\Phi = \Phi_2 - \Phi_1$$

$$T = \left|\frac{\overline{E}_{out}}{\overline{E}_{in}}\right|^2 = \left[\cos\left(\frac{\Delta\phi}{2}\right)\right]^2$$

The phase difference between the two arms carries the information about the substance to be detected.
One of the two arm is exposed to the analyte by means of a sensitive area.

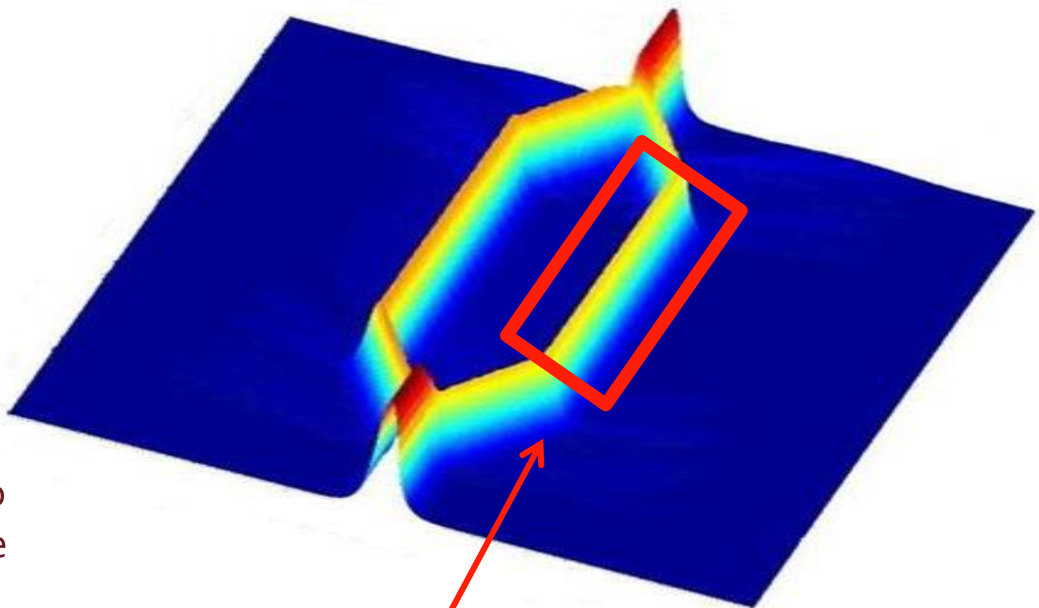

SENSITIVE AREA

Interrogation schemes

- Amplitude interrogation;
- Wavelength interrogation.

PHOTONICS RESEARCH GROUP

Mach – Zehnder Interferometer Sensors

Amplitude and Wavelength Interrogation

Output power varying sinusoidally depends on the concentration of the detecting substance

$$T = \left|\frac{\overline{E}_{out}}{\overline{E}_{in}}\right|^2 = \left[\cos\left(\frac{\Delta\Phi}{2}\right)\right]^2 = \left[\cos\left(\frac{\Delta\phi_0 + \Delta\phi}{2}\right)\right]^2$$

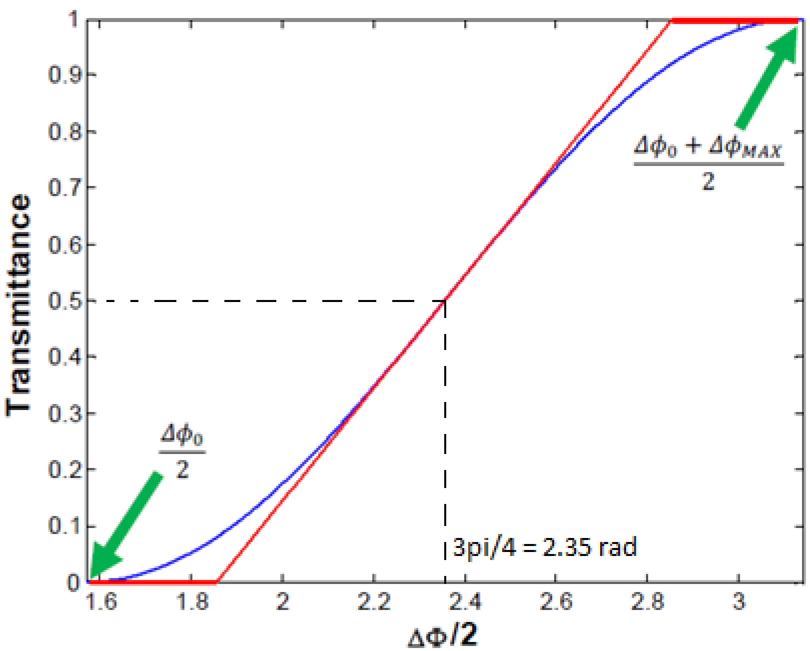

Zero-transmittance wavelength varying linearly with the concentration of the detecting substance/analyte

$$\Delta\lambda_{MZI} = \frac{\lambda_m}{\Delta n_{g,MZI}} S_w \Delta n_c$$

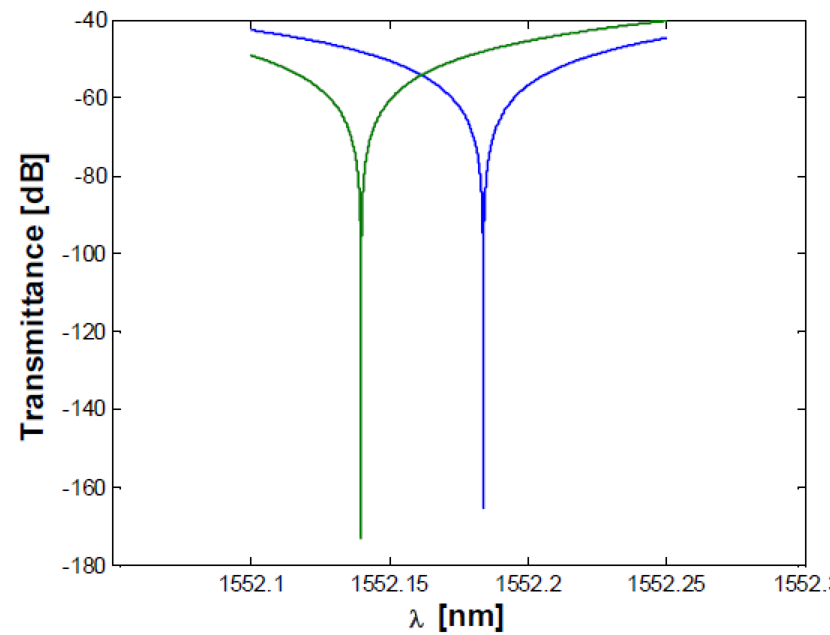

MZI wavelength shift can be Gs times the RR shift.

$$\frac{\Delta\lambda_{MZI}}{\Delta\lambda_{RING}} = \frac{n_{g,RING}}{\Delta n_{g,MZI}} = G_S = \frac{1}{1 - \frac{n_{g,2}}{n_{g,1}}}$$

PHOTONICS RESEARCH GROUP

Mach-Zehnder Enhanced Vernier Effect (RR-MZI)

Mixing architectures, Maximizing Performance

MZI Sensor → MZI-Enhanced Vernier Sensor ← Ring resonator

MZI-Enhanced Vernier Sensor

Improvement of MZI refractive index sensing performance compared to RR can be further boosted by cascading a RR and a MZI sensor in order to operate in the second regime of the Vernier effect.

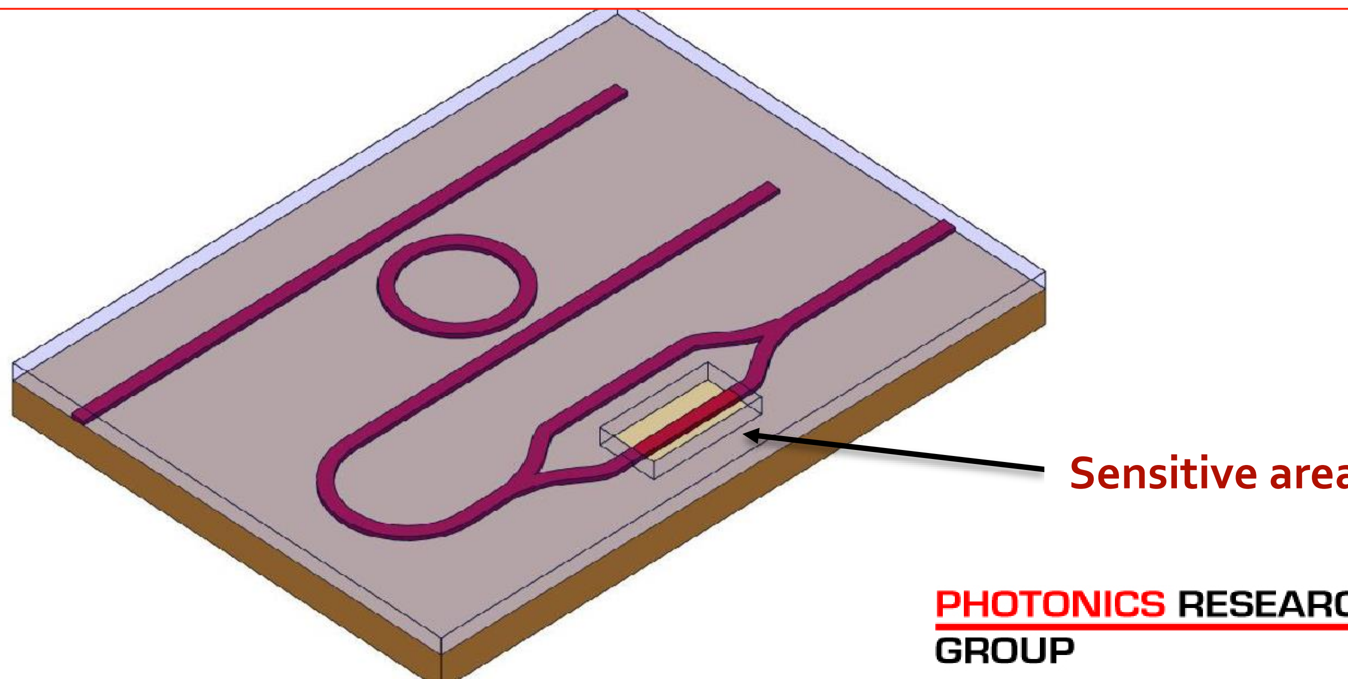

PHOTONICS RESEARCH GROUP

MACH-ZEHNDER ENHANCED VERNIER SENSORS

Mixing architectures, Maximizing Performance

Overall wavelength shift of RR-MZI sensors due to cladding refractive index variation:

$$\Delta\lambda_{tot} = \left(\frac{FSR_{tot}}{FSR_{MZI}}\right)\Delta\lambda_{MZI} = \left(\frac{FSR_{filter}}{\Delta FSR}\right)\Delta\lambda_{MZI} = G_A \cdot \frac{\lambda_m}{\Delta n_{g,MZI}} S_w \Delta n_c$$

Limit of detection (LOD) of RR-MZI sensors:

$$LOD = \frac{FSR_{filter} \cdot \Delta n_{g,MZI}}{G_A \cdot \lambda_m \cdot S_w} = \frac{\Delta FSR \cdot \Delta n_{g,MZI}}{\lambda_m \cdot S_w}$$

LOD of standard RR-RR Vernier:

$$LOD_{RR-RR} = \frac{\Delta FSR \times n_{g(RR)}}{\lambda_{res} S_w}$$

RR-MZI sensors can exhibit wavelength shifts 14 times larger as well as limits of detection 1 order of magnitude better than standard Vernier devices.

Performance parameters for the standard Vernier sensor and the MZI-Enhanced Vernier sensor with SU8 cladding.

Parameter	Standard Vernier sensor	MZI-Enhanced Vernier sensor
FSR_{filter}	2.791 nm	2.791 nm
FSR_{sensor}	2.776 nm	2.771 nm
ΔFSR	15.6 pm	19.8 pm
G_A	179.39	140.97
$\Delta\lambda_{tot}$*	3.4 nm	47.3 nm
LOD	$8 \cdot 10^{-5}$ RIU	$6 \cdot 10^{-6}$ RIU

* calculated with $\Delta n_c = 10^{-4}$

PHOTONICS RESEARCH GROUP

Mach-Zehnder Enhanced Vernier Sensors (RR-MZI)

Pros & Cons

+ Ultra high overall sensitivity;
+ Ultra low LOD;
+ Poor noise sensitivity;
+ Suitable for gas sensing;
+ Many design degrees of freedom.

– Larger bandwidth is required compared to standard Vernier architectures with cascaded ring resonators.

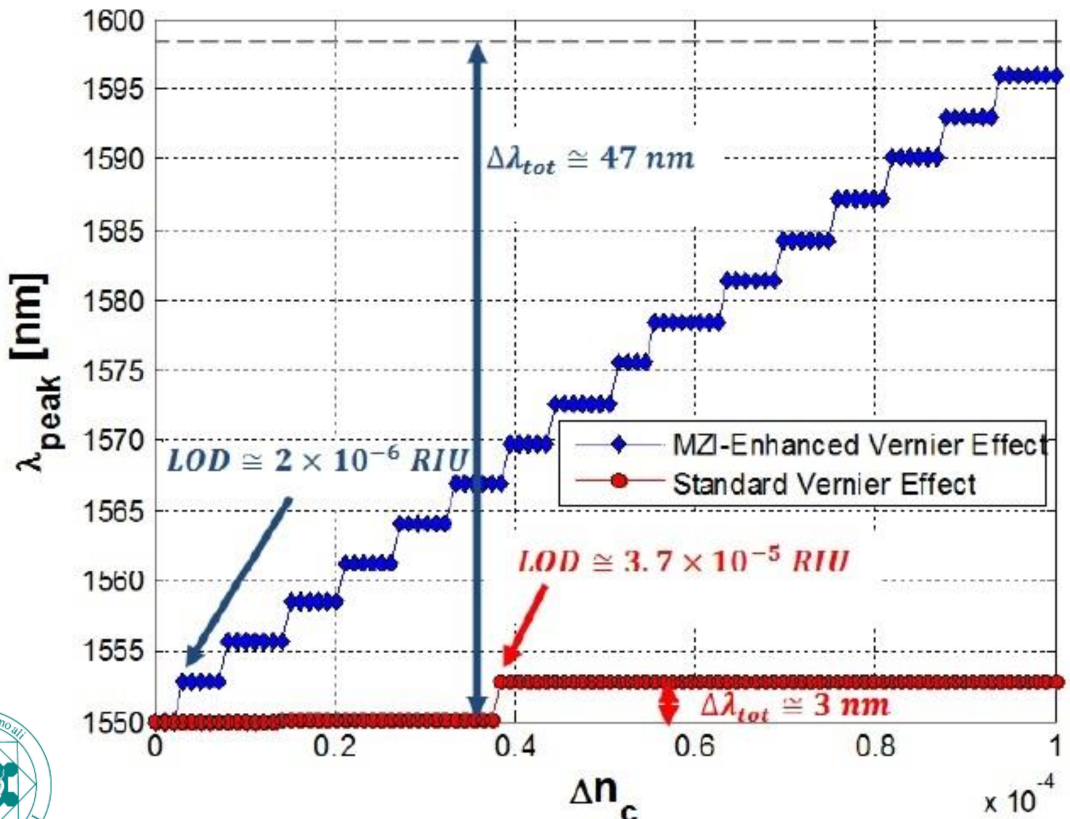

COMPARISON

Limit of detection and dynamic range of Vernier cascaded RR and RR-MZI photonic sensors.

Vernier RR-MZI can exhibit better refractive index sensing performance compared to standard RR Vernier sensors.

PHOTONICS RESEARCH GROUP

OUTLINE

- PHOTONIC SENSING APPLICATIONS

- PHOTONIC DEVICES FOR SENSING APPLICATIONS
  - Design of photonic waveguides;
  - Optical sensing principles;
  - Group IV material systems and alloys.

- **PHOTONIC ARCHITECTURES BASED ON VERNIER EFFECT**
  - The Vernier effect for photonic sensing;
  - Vernier sensors based on cascaded microring resonators;
  - Vernier sensors based on cascaded ring resonator and MZI;
  - **Vernier sensors based on cascaded ring resonator and MZI with a Sagnac loop.**

- ADVANCED PHOTONIC SENSORS OPERATING IN THE NEAR-IR AND MID-IR
  - Sensing principles for gas detection in the mid-IR;
  - Photonic sensors based on the Vernier effect for methane and ethane detection;
  - Experimental demonstration of the Vernier effect in integrated Photonics.

- CONCLUSIONS

RR-MZI Vernier Sensors with a Sagnac loop (RR-MZI-Sagnac)

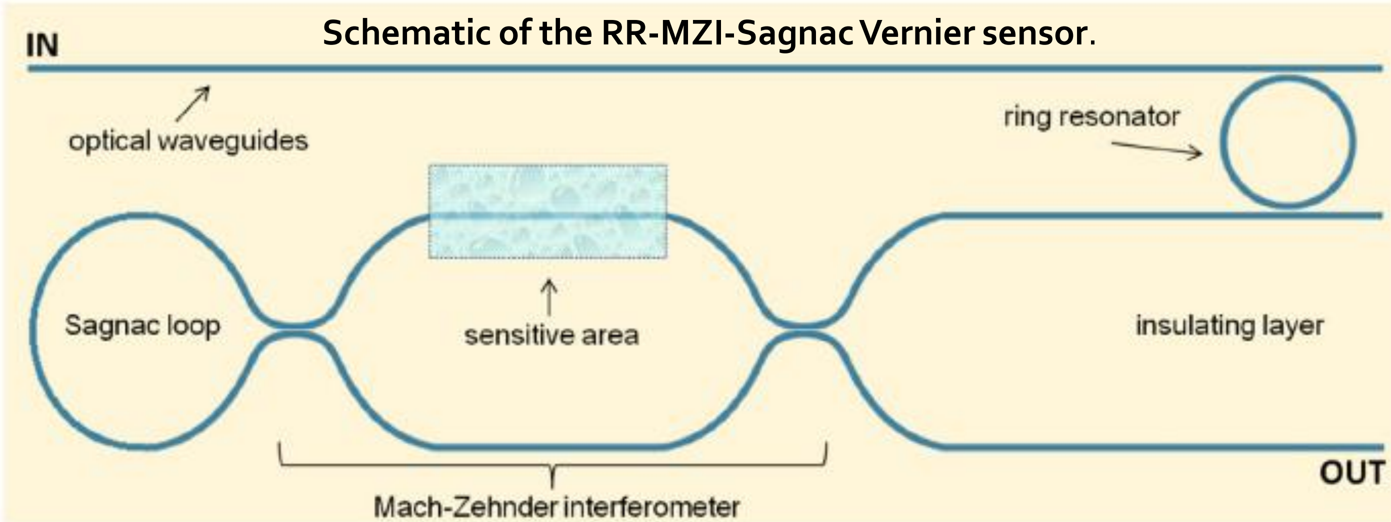

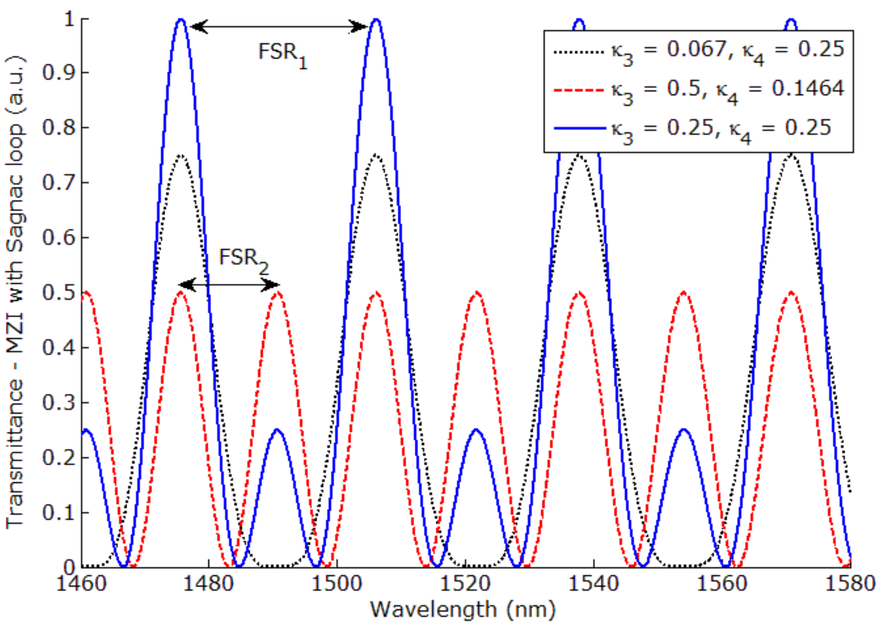

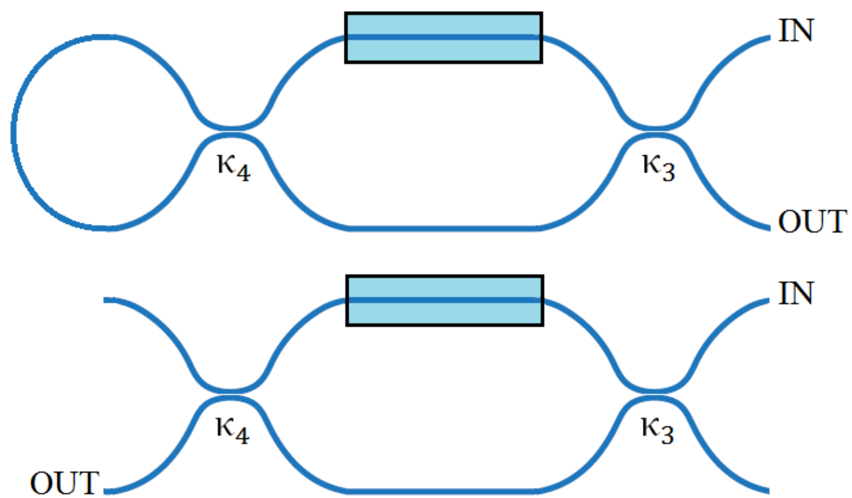

The FSR of the MZI with the Sagnac loop can be changed if compared to the standard MZI by optimized power coupling coefficients, k3 and k4.

PHOTONICS RESEARCH GROUP

RR-MZI and RR-MZI-Sagnac Vernier Sensors: Comparison

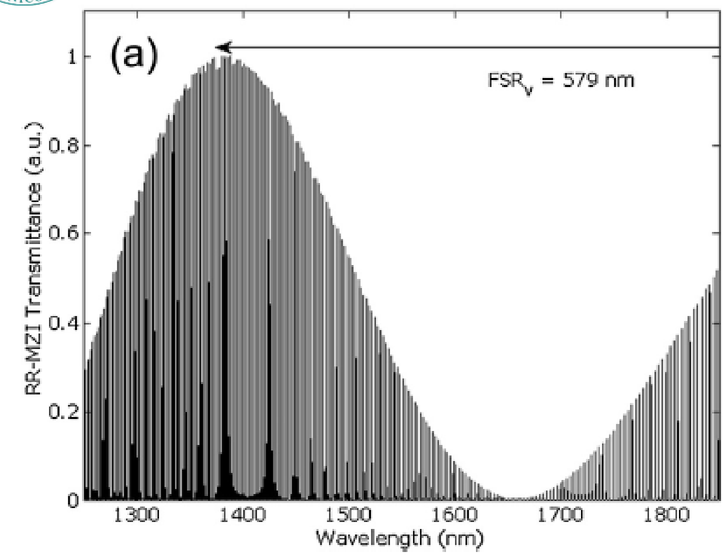

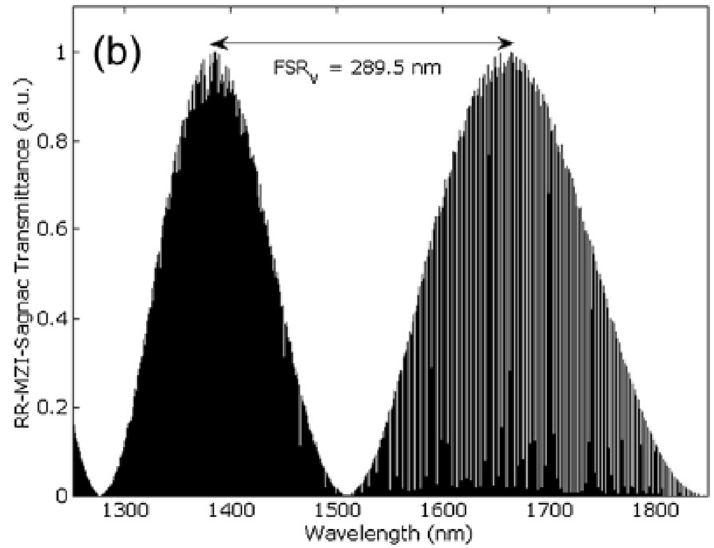

RR-MZI-Sagnac Vernier sensor with <u>balanced MZI</u>

The total Vernier FSR can be halved compared to RR-MZI sensors

Performance are comparable (same sensitivity, gain and LOD)

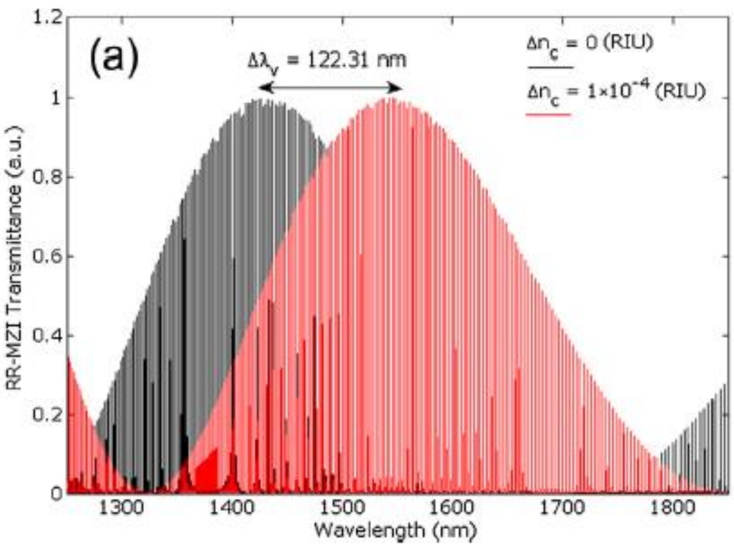

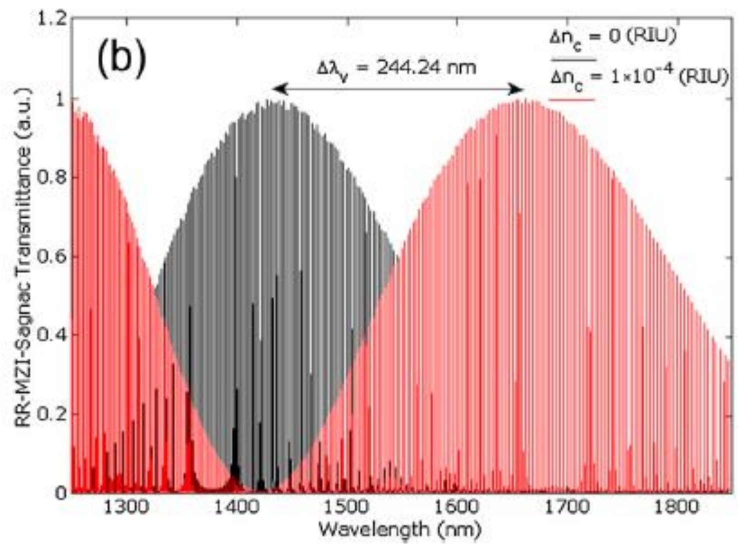

RR-MZI-Sagnac Vernier sensor with <u>unbalanced MZI</u>

The Vernier FSRs are comparable

Wavelength sensitivitiy can be double compared to RR-MZI sensors with the same bandwidth

RR-MZI **RR-MZI-Sagnac**

PHOTONICS RESEARCH GROUP

B. Troia, V. Passaro et al., Sens. Act. B, vol. 240, pp. 76-89 (2017).

RR-MZI Vernier Sensors with a Sagnac loop (RR-MZI-Sagnac)

Pros & Cons

+ Same RI performance as RR-MZI Vernier in half the bandwidth (balanced Sagnac- MZI);
+ Double RI performance than RR-MZI in the same bandwidth (unbalanced Sagnac- MZI);
+ Poor noise sensitivity;
+ Suitable for chemical and biochemical sensing;
+ Many design degrees of freedom;
+ To be experimentally verified.

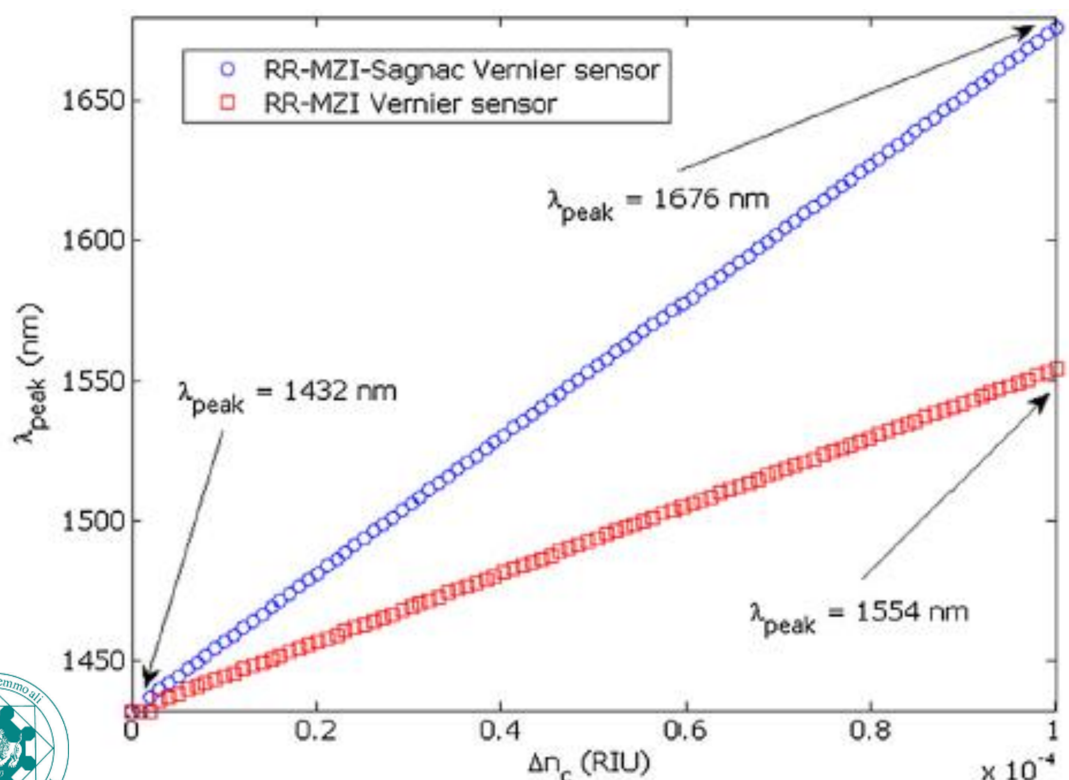

COMPARISON

Vernier RR-MZI-Sagnac can exhibit the same refractive index sensing performance of RR-MZI Vernier sensors in half the bandwidth (balanced MZI).

Vernier RR-MZI-Sagnac can exhibit double refractive index sensing performance compared to RR-MZI Vernier sensors within the same bandwidth (unbalanced MZI).

PHOTONICS RESEARCH GROUP

RR-MZI Vernier Sensors with a Sagnac Loop

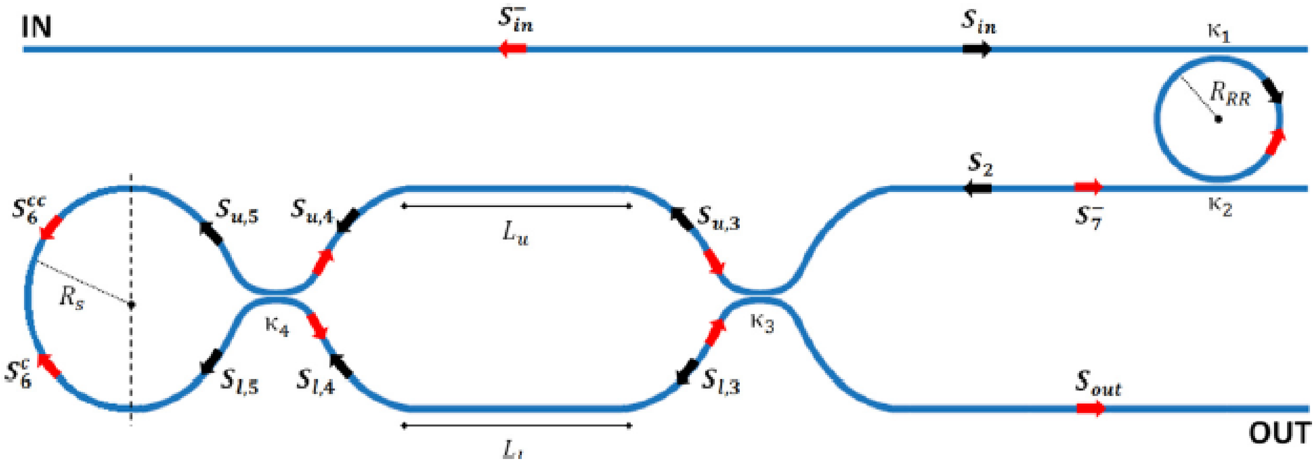

The contribution of counter-propagating signals can be minimized by optimal design of power coupling coefficient of the ring resonator (k1, k2).

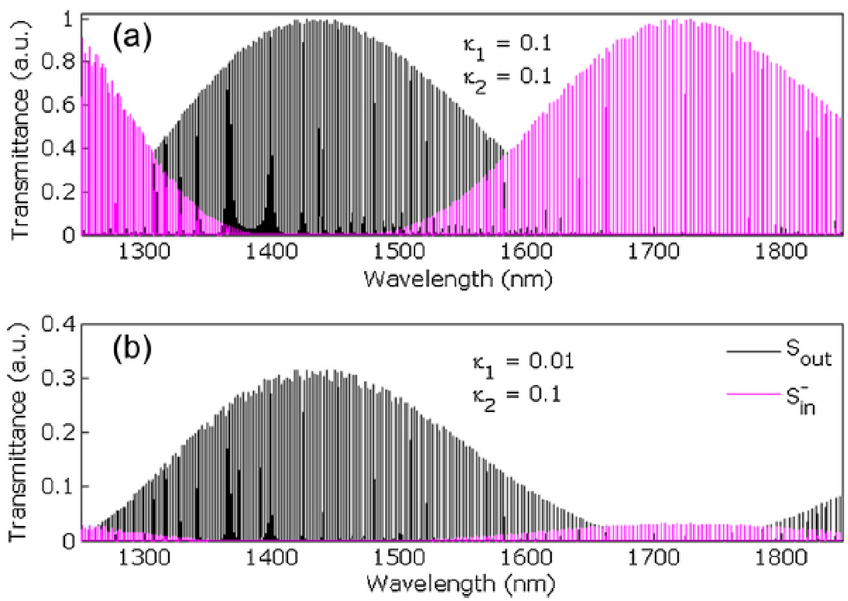

PHOTONICS RESEARCH GROUP

FANO SENSORS IN THE MID-INFRARED

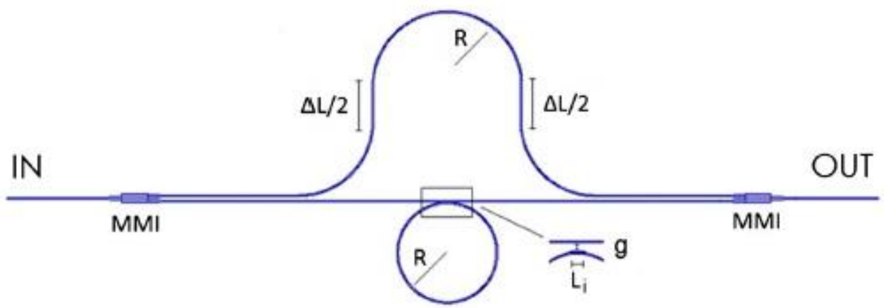

Schematic of a RR-coupled MZI device. Input/output waveguides and MMIz, the MZI and RR geometrical parameters are labeled.

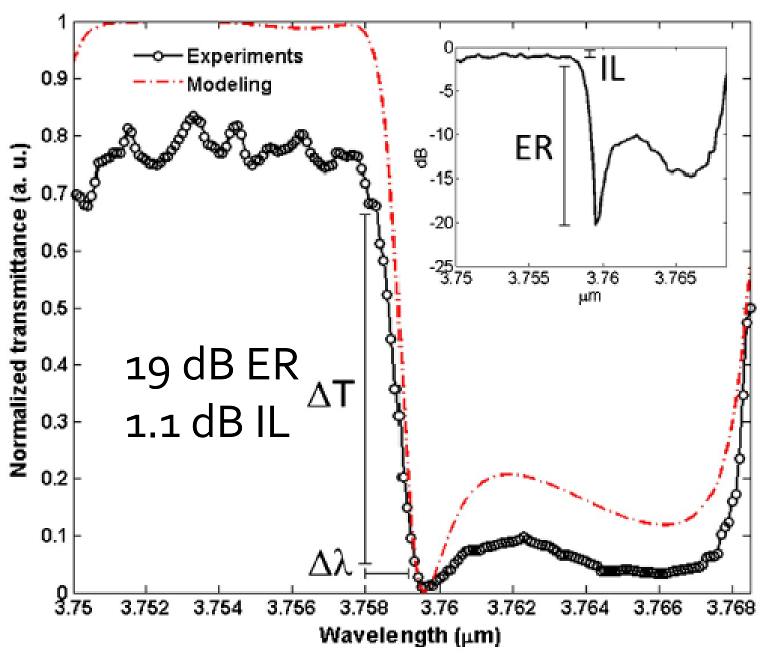

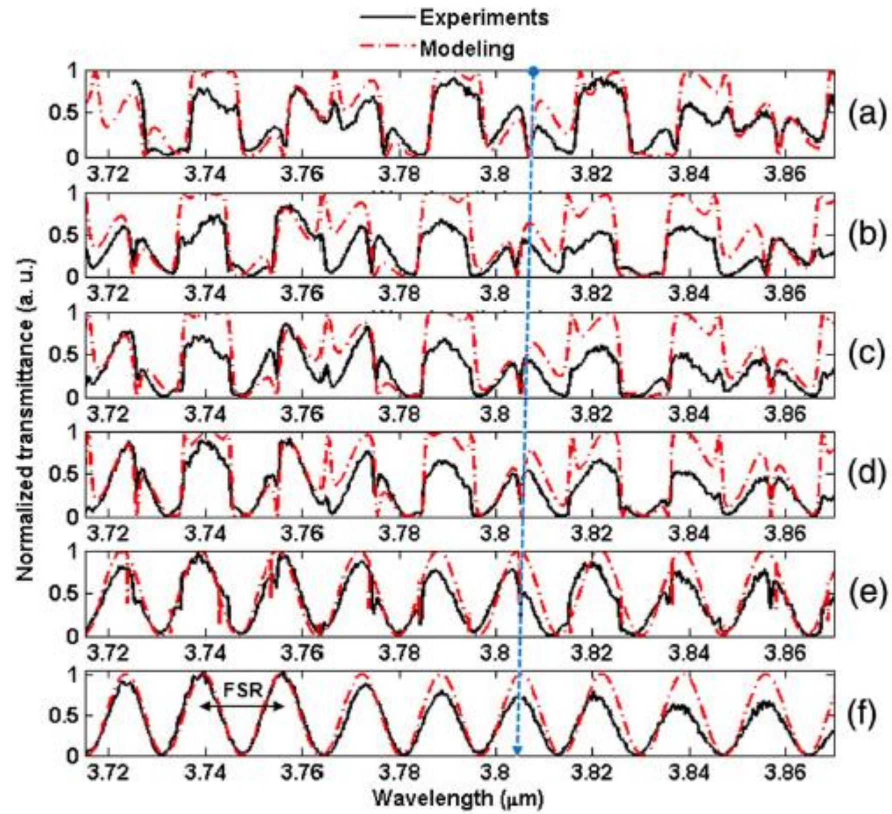

(**top**) Theoretical and experimental spectra of a Fano device in a broad spectral range as a function of different values of coupler gap g (a = 400 nm, b = 500 nm, c = 600 nm, d = 700 nm, e = 800 nm, f > 1000 nm).

(**left**) Zoomed plot of a Fano-shape resonance (g = 400 nm).

PHOTONICS RESEARCH GROUP

B. Troia et al., Appl. Opt., Vol. 56, no. 31, pp. 8769-8776 (2017).

PHOTONIC VERNIER SENSORS: READOUT TECHNIQUES

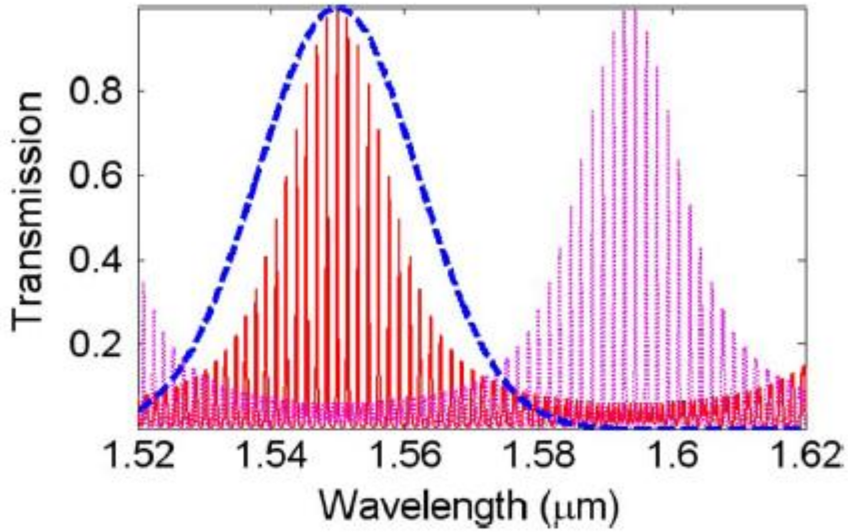

Spectral power distribution of a broadband source (dashed curve), and the transmission spectra of cascaded rings with slightly different FSRs when the envelope function has maximal (solid curve) and minimal (dotted curve) overlap with the source spectrum.

$$P_s = \int_0^\infty [P_i(\lambda) T_r(\lambda) T_s(\lambda)] d\lambda$$

Intensity readout scheme:

A low-cost broadband source (e.g., LED) can be used to this purpose. The overlapping integral between the LED spectral power distribution and the Vernier ones, can be used for the detection.

Photonic Vernier Sensors: readout techniques

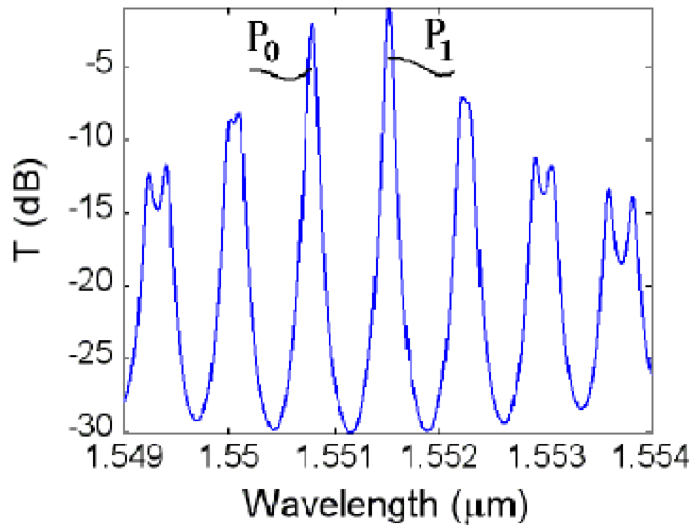

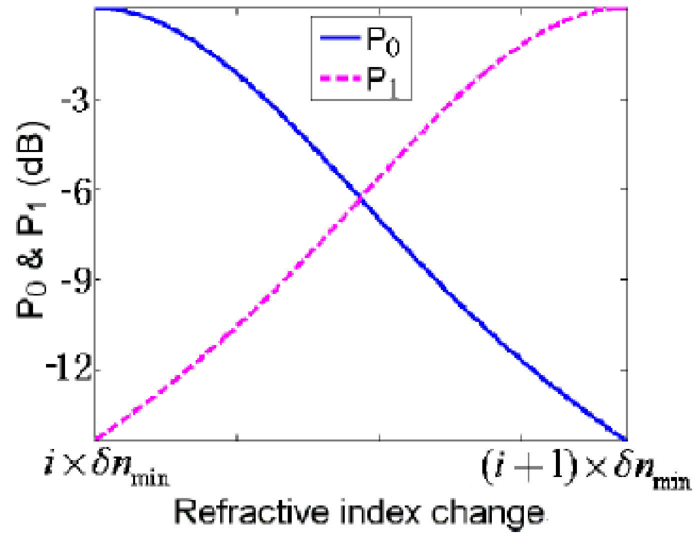

Wavelength readout scheme:

A sophisticated and generally expensive OSA (optical spectrum analyzer) can be used for detecting P_0 and P_1.
The sensitivity can be enhanced up to three orders of magnitude.

Other approaches:

- Use of a <u>reference</u> Vernier device to be cascade-coupled to that employed for sensing purposes. Integrated microheaters on the «sensing» ring resonator of the <u>reference</u> device can generate Vernier peak wavelength shifts opposite to those of the sensing Vernier architecture.

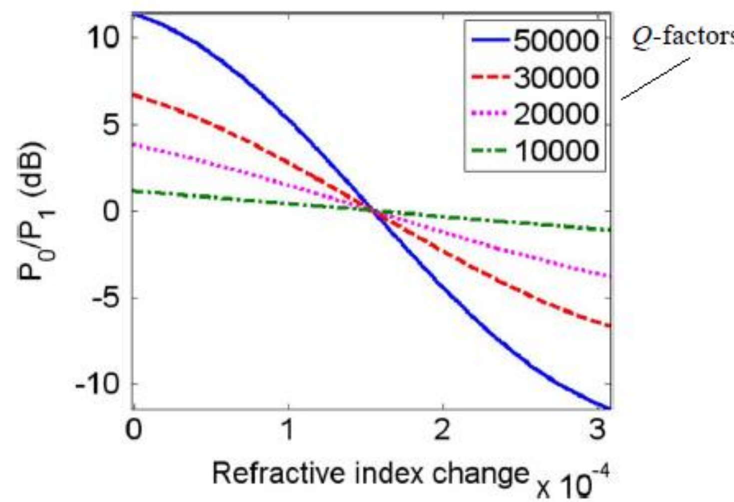

PHOTONICS RESEARCH GROUP

OUTLINE

- PHOTONIC SENSING APPLICATIONS

- PHOTONIC DEVICES FOR SENSING APPLICATIONS
  - Design of photonic waveguides;
  - Optical sensing principles;
  - Group IV material systems and alloys.

- PHOTONIC ARCHITECTURES BASED ON VERNIER EFFECT
  - The Vernier effect for photonic sensing;
  - Vernier sensors based on cascaded microring resonators;
  - Vernier sensors based on cascaded ring resonator and MZI;
  - Vernier sensors based on cascaded ring resonator and MZI with a Sagnac loop.

- **ADVANCED PHOTONIC SENSORS OPERATING IN THE NEAR-IR AND MID-IR**
  - Sensing principles for gas detection in the mid-IR;
  - Photonic sensors based on the Vernier effect for methane and ethane detection;
  - Experimental demonstration of the Vernier effect in integrated Photonics.

- CONCLUSIONS

DESIGN OF PHOTONIC GAS SENSORS OPERATING IN THE MID-IR

Explosion limits of harmful gases

Gas	Lower Explosive Limit LEL (%)	Upper Explosive Limit UEL (%)
Butane (C_4H_{10})	1.8	8.4
Carbon monoxide (CO)	12.5	74.0
Methane (CH_4)	**5.0**	**15.0**
Ethane (C_2H_6)	3.0	12.5
Propane (C_3H_8)	2.1	9.5

Optical sensing principles

Homogeneous sensing

$$n_{mixture} = n_{gas} \cdot C_{gas} + n_{air} \cdot C_{air}$$
$$C_{air} = 1 - C_{gas}$$

linear approximation

CH_4 refractive index = 1.000444 @ 3.39μm
Air refractive index = 1 @ 3.39μm

Methane (CH_4)	C_{CH4}	C_{air}	$n_{mixture}$
LEL = 5%	0.05	0.95	1.0000222
UEL = 15%	0.15	0.85	1.0000666

Design requirements

- $\Delta n_{c,min}$ = 2.22×10^{-5} RIU (*limit of detection* – LOD)
- $\Delta n_{c,max}$ = 6.66×10^{-5} RIU

Optical absorption

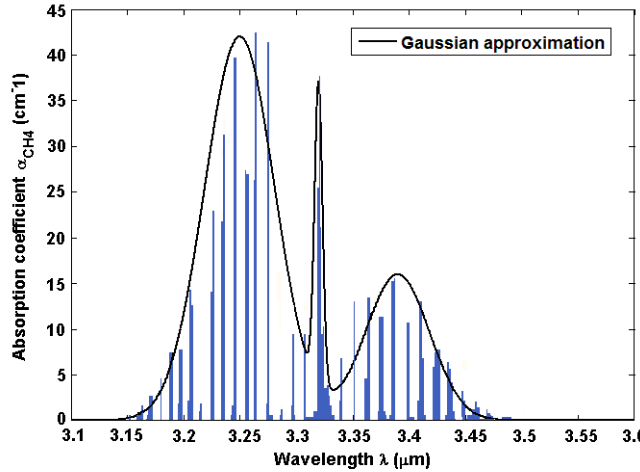

$$I = I_0 \exp(-\alpha_{gas} L_{sensore}); \ \ \alpha_{gas} = \varepsilon C_{gas}$$
$$\alpha_{tot} = \alpha + C_{gas} \cdot \Gamma_s \cdot \alpha_{gas}(\lambda) + C_{air} \cdot \Gamma_s \cdot \alpha_{air}(\lambda)$$

PHOTONICS RESEARCH GROUP

Application of the desing tool: Vernier devices for gas sensing

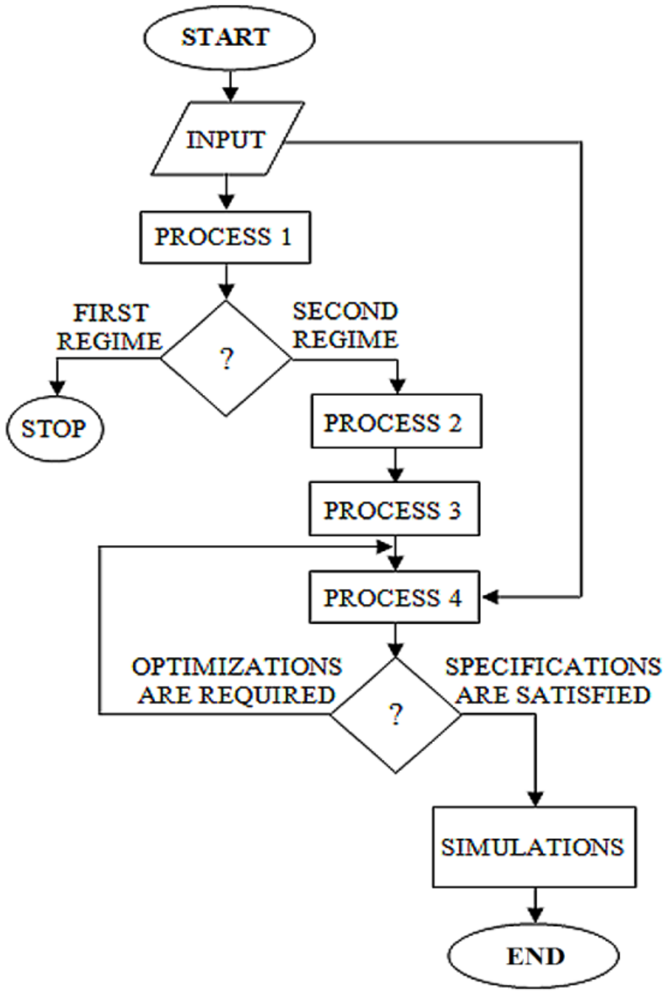

Flowchart of the algorithmic procedure developed for the design of ultra-high performance Vernier photonic sensors

Homogeneous sensing

$$n_{mix} = n_{gas} \cdot C_{gas} + n_{air} \cdot C_{air}, \text{ with } C_{air} = 1 - C_{gas}$$

EL_{CH_4}	C_{CH_4}	C_{air}	n_{mix}
LEL = 5%	0.05	0.95	1.00002185
UEL = 15%	0.15	0.85	1.00006555

$$\Delta n_{c,min} = n_{CH_4,LEL} - n_{air} = 2.185\times10^{-5} \text{ RIU};$$
$$\Delta n_{c,max} = n_{CH_4,UEL} - n_{air} = 6.555\times10^{-5} \text{ RIU}.$$

Absorption based sensing:

Methane absorption spectrum in the MIR.

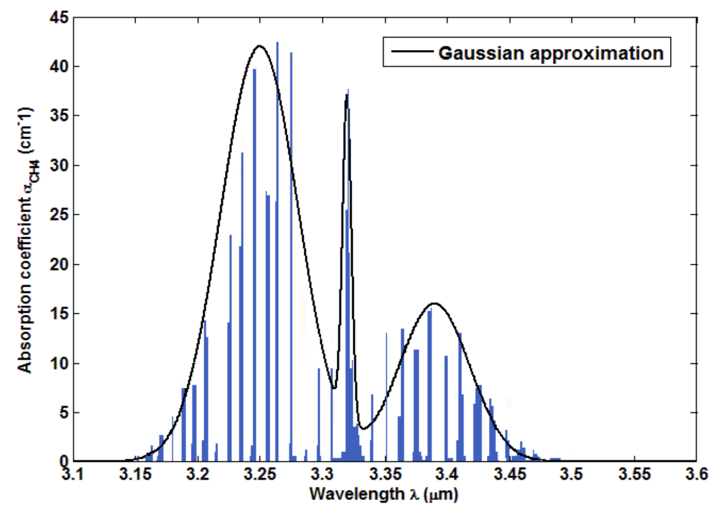

$$\alpha_{mix} = \alpha_{gas}(\lambda) \cdot C_{gas} \cdot \Gamma_c + \alpha_{air}(\lambda) \cdot C_{air} \cdot \Gamma_c$$

PHOTONICS RESEARCH GROUP

DESIGN OF PHOTONIC GAS SENSORS OPERATING IN THE MID-IR

Operation of the SINGLE RING RESONATOR supposed to be exposed to a CH_4 concentration of 15%

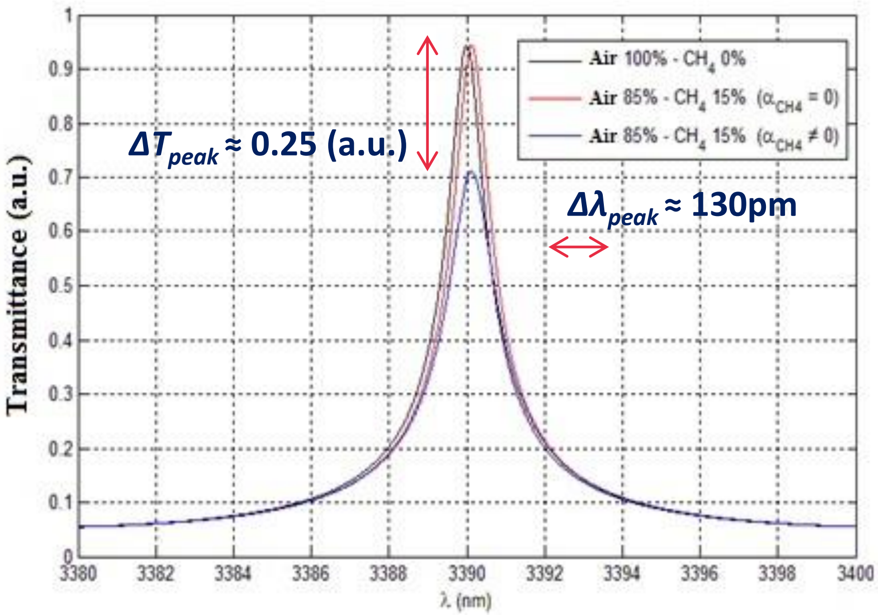

Cavity length ≈ 270μm

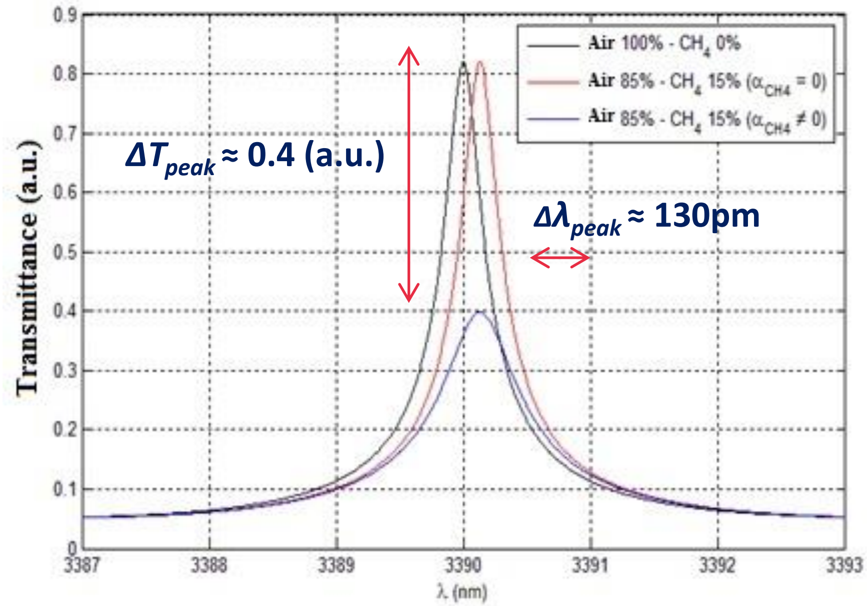

Cavity length ≈ 1000μm

Performance

$$S_\lambda = S_W \frac{\lambda}{n_{eff}^0} = 1966 \left(\frac{nm}{RIU} \right) \qquad LOD = \frac{\Delta\lambda}{S_\lambda} = 4.0694 \times 10^{-5} \left(RIU \right)$$

Minimum resolution assumed for the optical spectrum analyzer (OSA): Δλ = 80pm

Comment

The wavelength shift of the resonant peak calculated in case of a methane concentration of 5 % is lower than 80 pm, but it can be still detected by a high performance OSA !

In addition, the LOD achieved by this sensor does not satisfy design requirements (LOD = 2.22×10^{-5} RIU) !

PHOTONICS RESEARCH GROUP

Design of photonic gas sensors operating in the Mid-IR

$\Delta\lambda_{peak}$ = 0nm
Reference @ 3.39µm

$\Delta\lambda_{peak}$ = 9nm

Methane (CH_4) signature

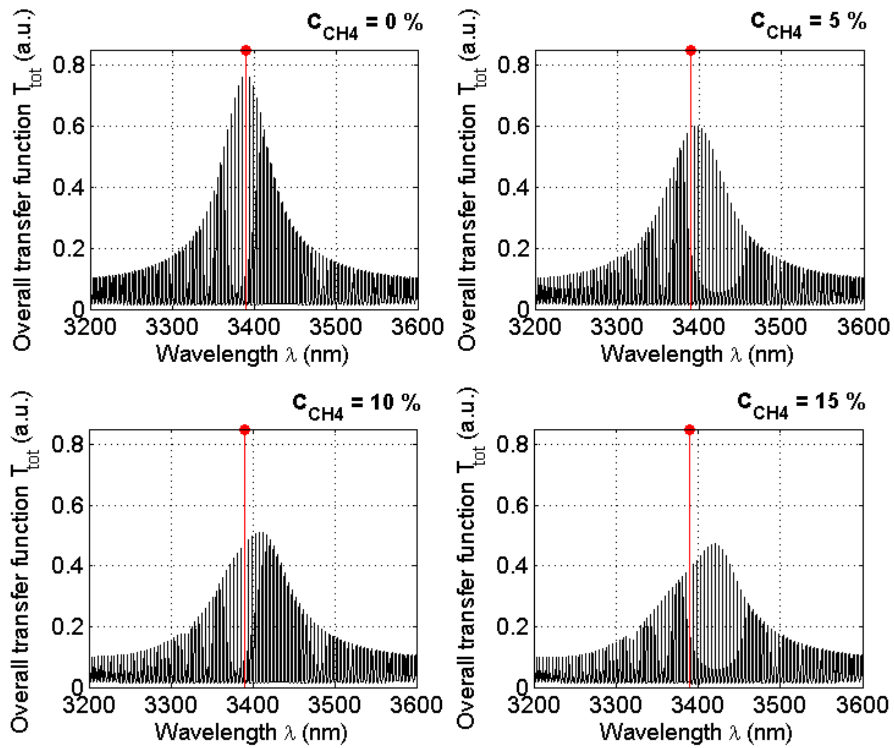

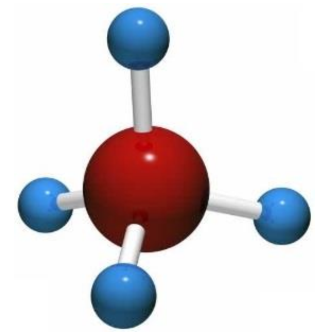

METHANE

$\Delta\lambda_{peak}$ = 18nm

$\Delta\lambda_{peak}$ = 31nm

Comparison between theoretical results of single ring resonator and photonic sensor based on the Vernier effect:

Performance	Single ring resonator	Vernier sensor
S_λ	1.966 µm/RIU	224.4 µm/RIU
$\Delta\lambda$	†0.130 nm	*4.982 nm
FSR_{tot}	6.5825 nm	484.3 nm
LOD	4.0694×10^{-5} RIU	1.9568×10^{-5} RIU

† *induced by* $\Delta n_c = 6.66\times10^{-5}$ RIU
**induced by* $\Delta n_c = 2.22\times10^{-5}$ RIU

PHOTONICS RESEARCH GROUP

DESIGN OF PHOTONIC GAS SENSORS OPERATING IN THE MID-IR

Operation of the photonic sensor based on the Vernier effect as a function of different methane concentrations

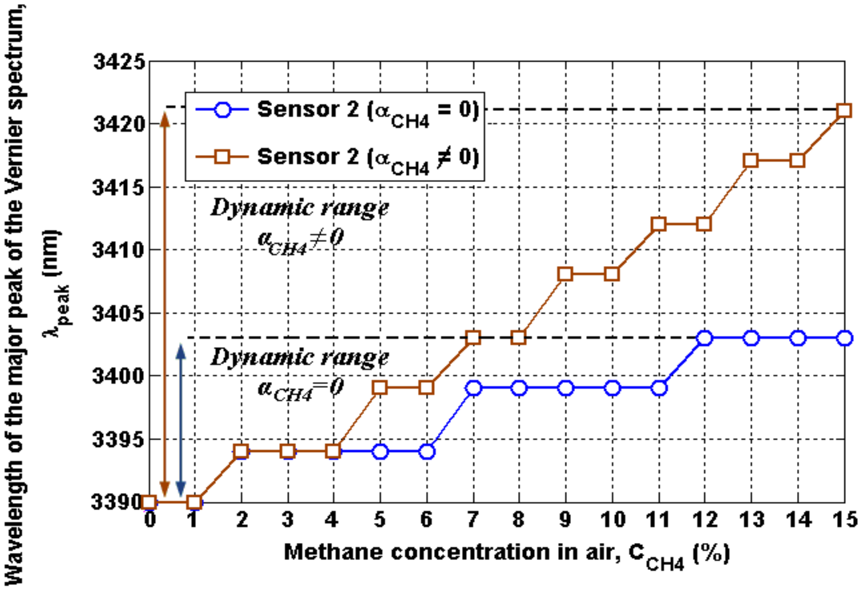

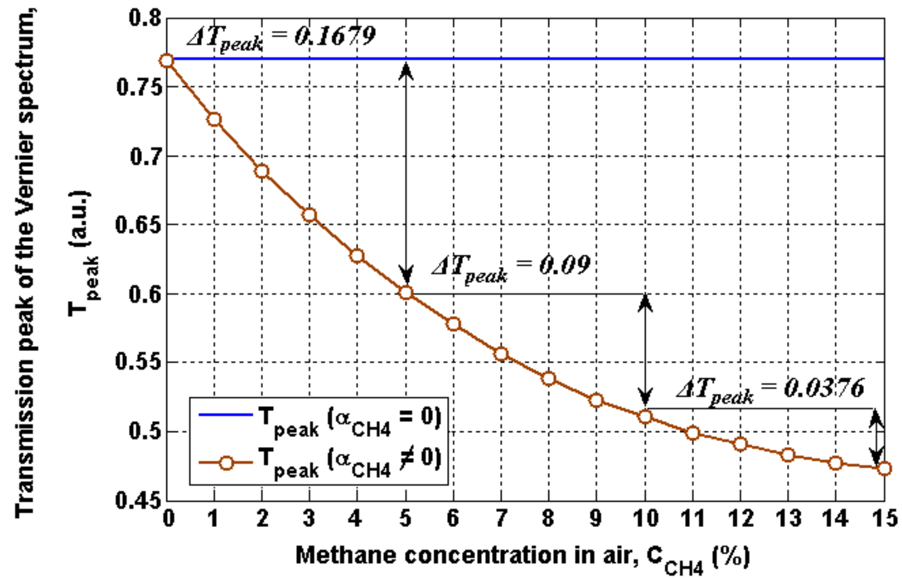

"Digital" sensor

($\alpha CH_4 = 0$)

- Dynamic range = 13nm;
- Number of quantization levels = 4;

($\alpha CH_4 \neq 0$)

- Dynamic range = 31nm;
- Number of quantization levels = 8;

Design parameters	Numerical results
L_{filter}	1200.4 µm
L_{sensor}	1516.25 µm
$\Delta n_{c,min}$	**1.9568×10^{-5} RIU**
$\Delta n_{c,max}$	**2.158×10^{-3} RIU**
ΔFSR	39.46 pm
$S_{\lambda,tot}$	**224.4 µm/RIU**
FSR_{tot}	484.3 nm
$\Delta\lambda_{tot}$	**4.982 nm (induced by $\Delta n_c = 2.22\times10^{-5}$)**
G	**111.3**

PHOTONICS RESEARCH GROUP

Design of photonic gas sensors operating in the mid-IR

Explosion limits of harmful gases

Gas	LEL (%)	UEL (%)
Butane (C_4H_{10})	1.8	8.4
Carbon monoxide (CO)	12.5	74.0
Methane (CH_4)	5.0	15.0
Ethane (C_2H_6)	3.0	12.5
Propane (C_3H_8)	2.1	9.5

Optical sensing principles

Homogeneous sensing

$$n_{mixture} = n_{gas} \cdot C_{gas} + n_{air} \cdot C_{air}$$
$$C_{air} = 1 - C_{gas}$$

linear approximation

C2H6 refractive index = 1.00076 @ 3.39µm

Air refractive index = 1 @ 3.39µm

Ethane (C_2H_6)	C_{C2H6}	C_{air}	$n_{mixture}$
LEL = 3%	0.03	0.97	1.0000228
UEL = 12.5%	0.125	0.875	1.000095

Design requirements

- **$\Delta n_{c,min}$ = 2.28×10^{-5} RIU (*limit of detection* – LOD)**
- **$\Delta n_{c,max}$ = 9.5×10^{-5} RIU**

Optical absorption

Ethane absorption spectrum in mid-IR

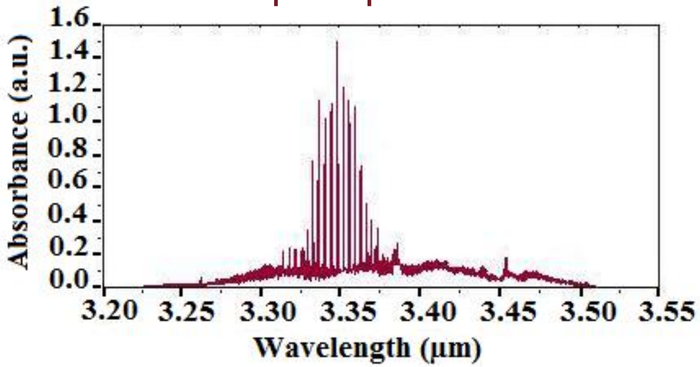

$$I = I_0 \exp(-\alpha_{gas} L_{sensore}); \;\; \alpha_{gas} = \varepsilon C_{gas}$$
$$\alpha_{tot} = \alpha + C_{gas} \cdot \Gamma_s \cdot \alpha_{gas}(\lambda) + C_{air} \cdot \Gamma_s \cdot \alpha_{air}(\lambda)$$

PHOTONICS RESEARCH GROUP

DESIGN OF PHOTONIC GAS SENSORS OPERATING IN THE MID-IR

Ethane (C2H6) signature

$\Delta\lambda_{peak}$ = 0nm
Reference @ 3.39µm

$\Delta\lambda_{peak}$ = 9nm

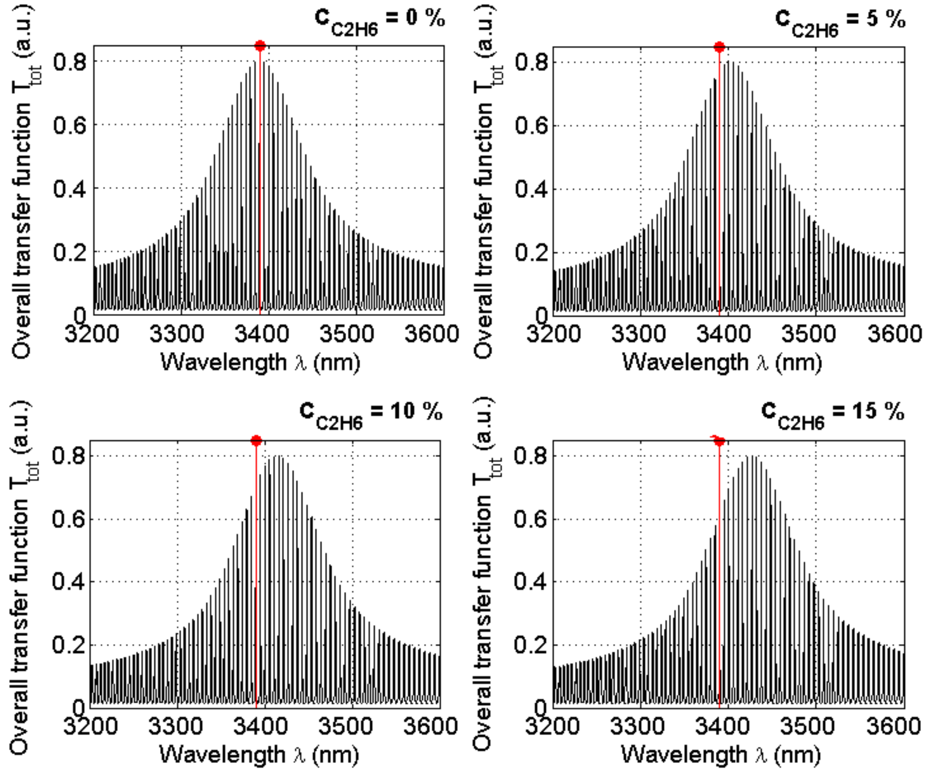

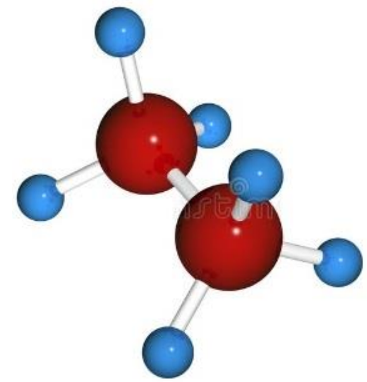

ETHANE

$\Delta\lambda_{peak}$ = 18nm

$\Delta\lambda_{peak}$ = 27nm

PHOTONICS RESEARCH GROUP

de' remi facemmo ali
1990
POLITECNICO DI BARI

Design of photonic gas sensors operating in the mid-IR

Operation of the photonic sensor based on the Vernier effect as a function of different ethane concentrations

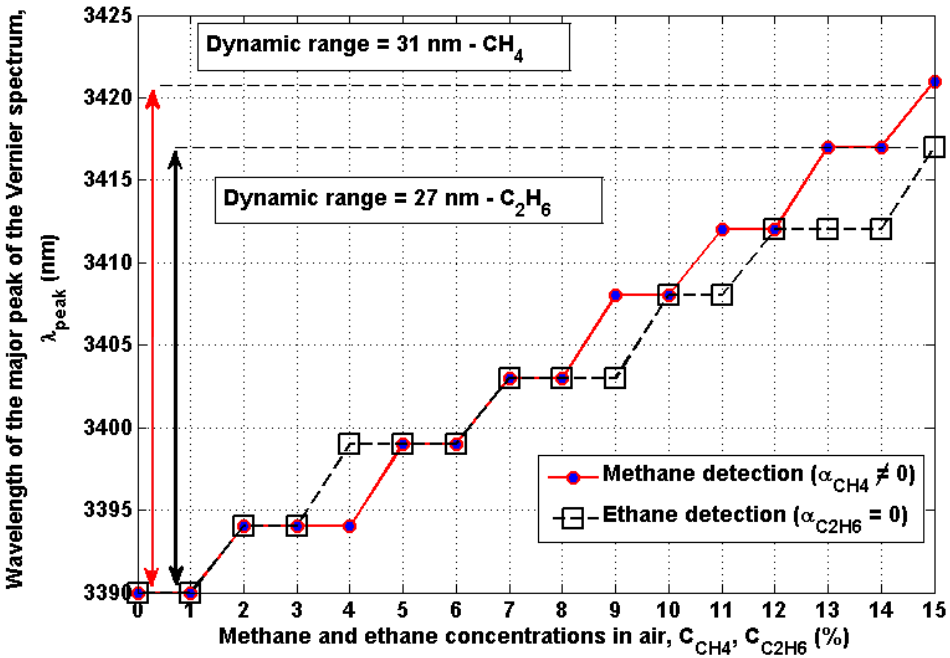

Design parameters	Numerical results
L_{filter}	1200.4 µm
L_{sensor}	1516.25 µm
$\boldsymbol{\Delta n_{c,min}}$	**2.0096×10^{-5} RIU**
$\boldsymbol{\Delta n_{c,max}}$	**2.2163×10^{-3} RIU**
ΔFSR	39.46 pm
$\boldsymbol{S_{\lambda,tot}}$	**218.51 µm/RIU**
FSR_{tot}	484.3 nm
$\boldsymbol{\Delta\lambda_{tot}}$	**4.982 nm (induced by Δn_c = 2.28×10^{-5})**
G	**111.3**

"Digital" sensor

(αC2H6 = 0)

- Dynamic range = 27nm;
- Number of quantization levels = 7;

PHOTONICS RESEARCH GROUP

DESIGN AND FABRICATION OF SOI RIB WAVEGUIDES OPERATING IN THE MID-IR (IN COLLABORATION WITH ORC – UNIVERSITY OF SOUTHAMPTON)

SOI rib waveguide designed at λ = 3.75 μm (H = 220 nm).

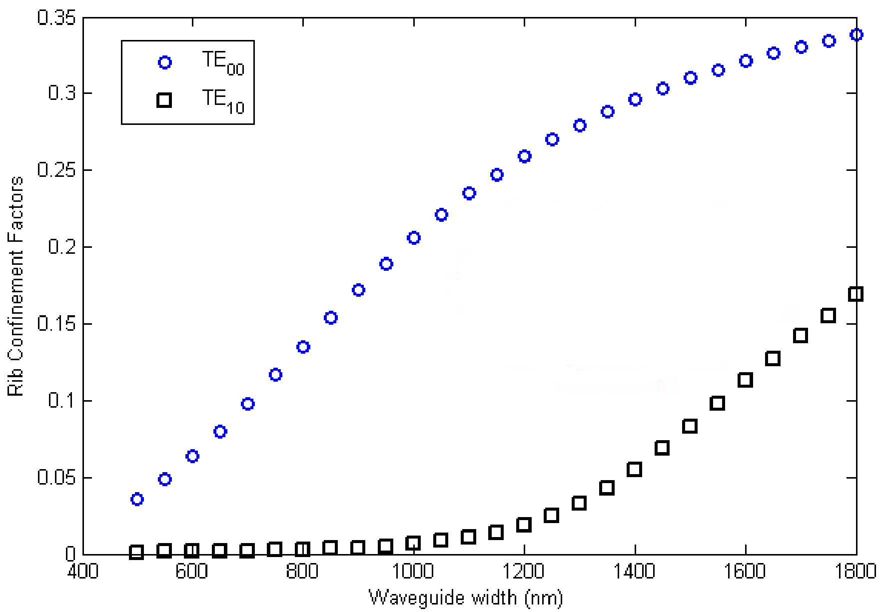

SEM image of a SOI rib waveguide.

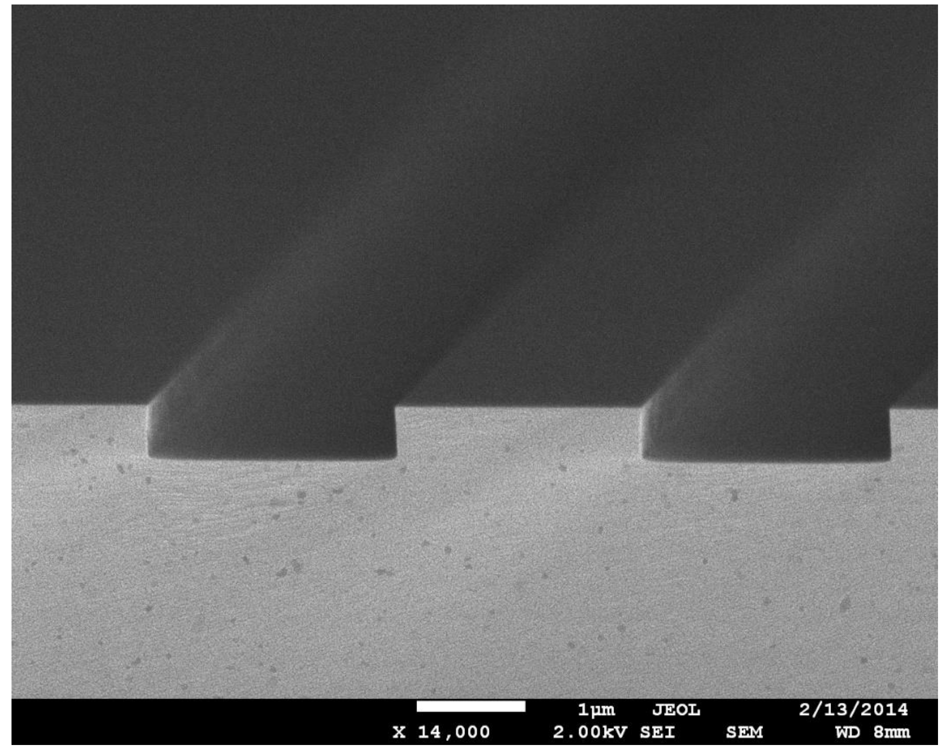

Real waveguide dimensions after the fabrication:

- 407 nm-thick Si top layer (*h*);
- Etch depth of 234 nm (*d*);
- Silicon slab of 173 nm;
- Sidewall tilting angle ≈ 90°.

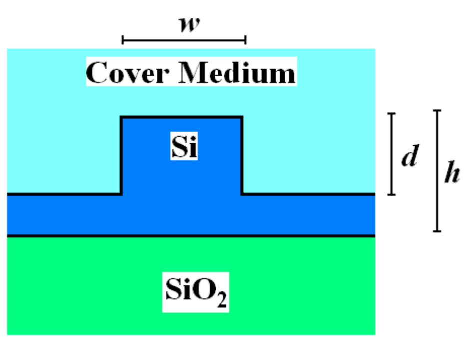

$$\alpha = 1.46 \pm 0.2 \ \frac{dB}{cm} \ @ \ 3.77 \ \mu m$$

PHOTONICS RESEARCH GROUP

DESIGN OF SOI DIRECTIONAL COUPLERS BASED ON RIB WAVEGUIDES OPERATING IN THE MID-IR

3D map of the power coupling coefficient as a function of fabrication tolerances

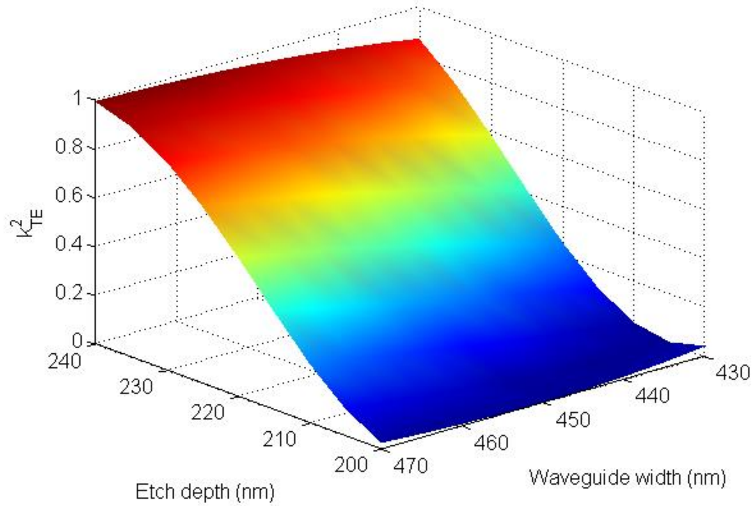

SOI directional couplers based on rib waveguides and designed at λ = 3.75 μm [4].

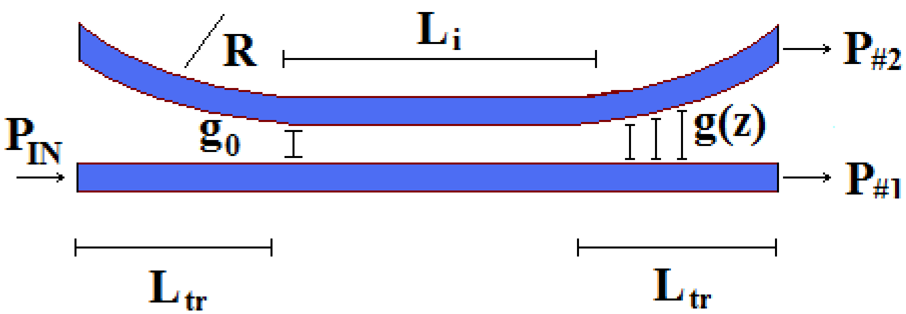

- g_0 is the constant directional coupler gap in the coupling region;
- L_i is the interaction length;
- R is the ring resonator radius;
- L_{tr} is the transition length (¾ R);
- $g(z)$ is the z-dependent directional coupler gap in the transition region;

2D map of the power coupling coefficient as a function of the directional coupler gap g_0.

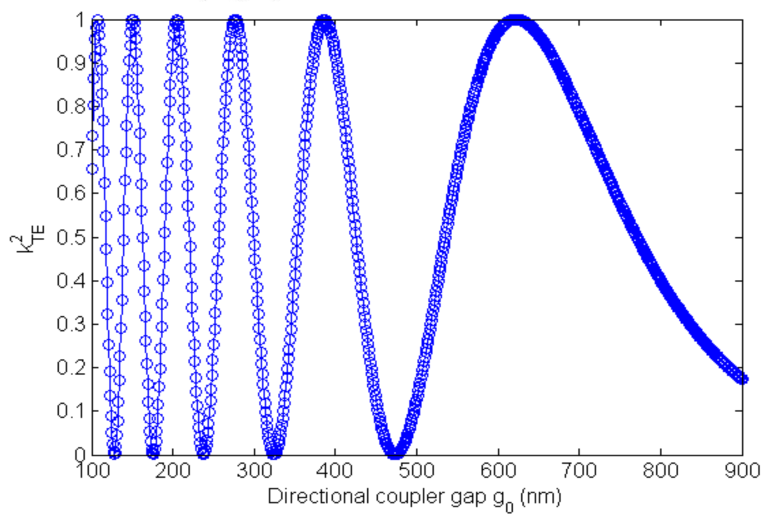

PHOTONICS RESEARCH GROUP

Experimental results of SOI directional couplers based on rib waveguides operating in the mid-IR (~3.8 m) and near-IR

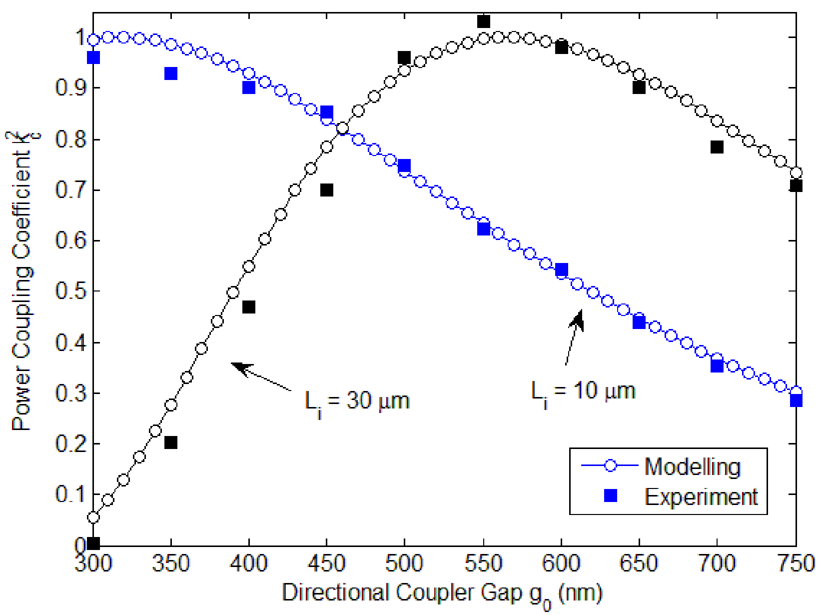

Mid-Infrared

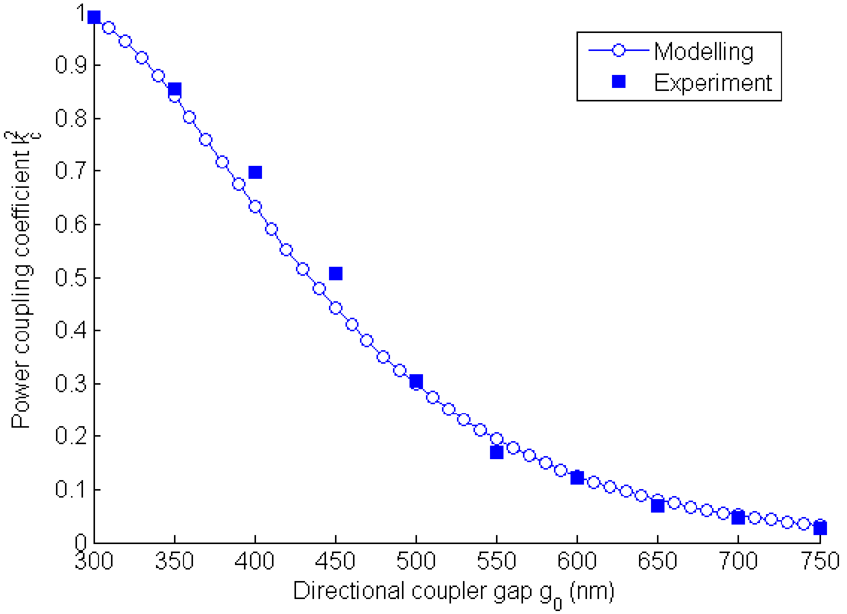

Near-Infrared (Li = 10 μm)

DESIGN AND FABRICATION OF RING RESONATORS IN THE MID-IR

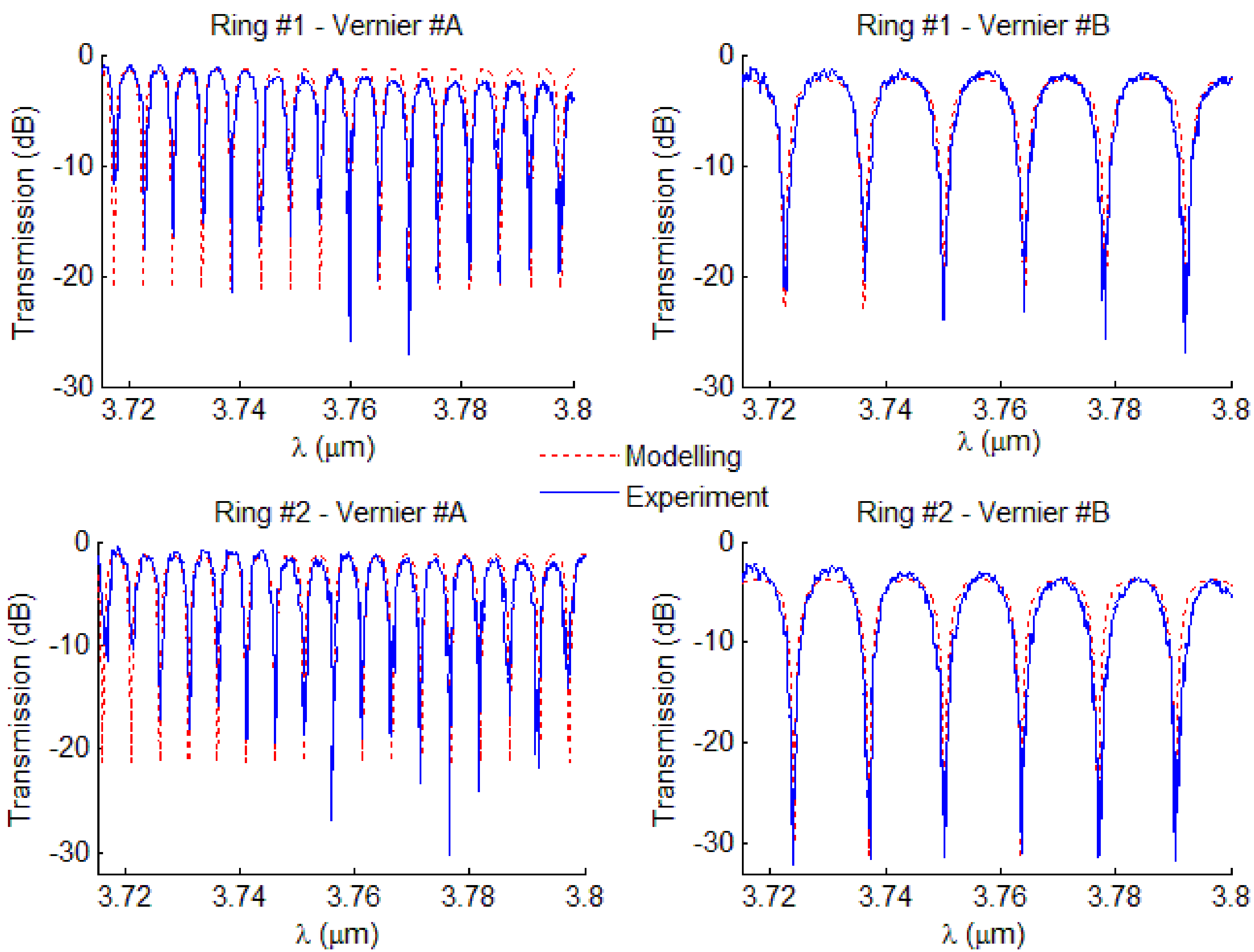

PHOTONICS RESEARCH GROUP

Design and fabrication of ring resonators in the mid-IR

Parameters	Vernier #A		Vernier #B	
Racetrack label	Ring #1	Ring #2	Ring #1	Ring #2
FSR (nm)	5.33	5.06	13.94	13.20
L (µm)	714	753.5	274	284
R (µm)	98	104	42	43
L_i (µm)	49.2	50	5	7
g_o (nm)	900	900	300	300
IL_{avg} (dB)	1.77	1.33	1.48	3.1
ER_{max} (dB)	25	29	25	30
Q-factor	~ 2,900	~ 2,500	~ 940	~ 850
$\Delta\lambda_{FWHM}$ (nm)	1.9	1.5	3.8	4.4

Vernier A: n = 19

18/19 = 0,947

(control over the third decimal digit)

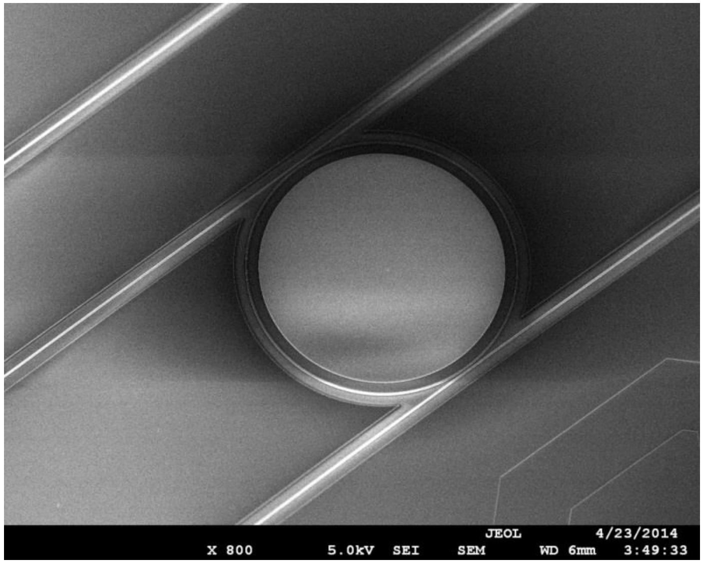

Scanning Electron Microscope (SEM) representative image of a ring resonator

Vernier B: n = 28

27/28 = 0,964

$$\frac{FSR''}{FSR'} = \frac{L'}{L''} = \frac{n-1}{n}$$

PHOTONICS RESEARCH GROUP

dè remi facemmo ali · POLITECNICO DI BARI · 1990

CASCADE-COUPLED RACETRACK RESONATORS IN THE MID-IR

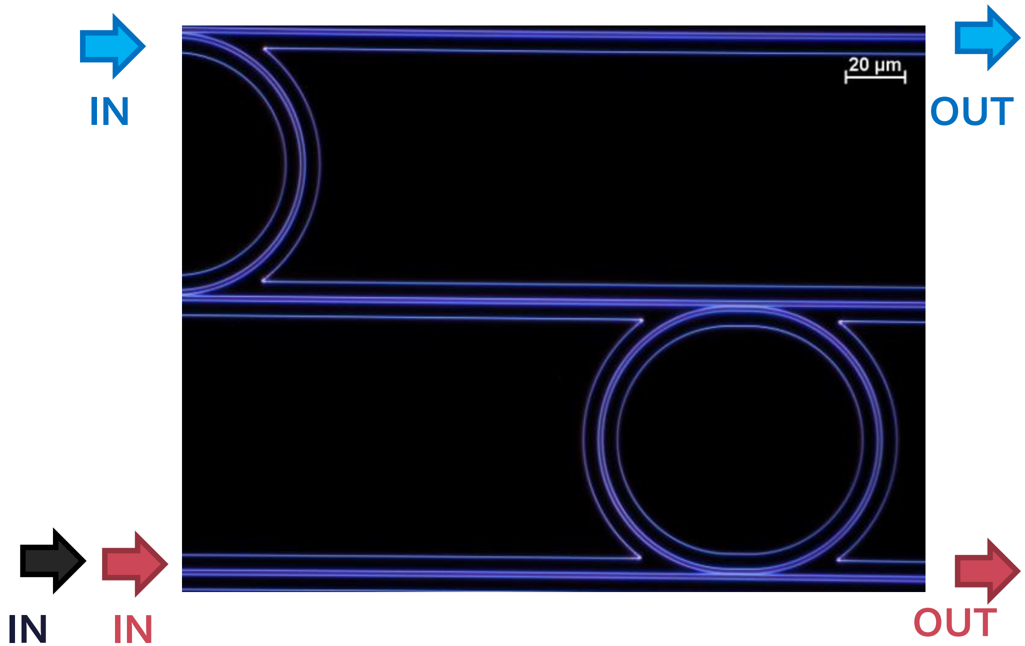

Legend:

- Sensing ring
- Filtering ring
- Vernier

Fabrication of devices at ORC (Southampton) by:

1) e-beam lithography
2) dry etching

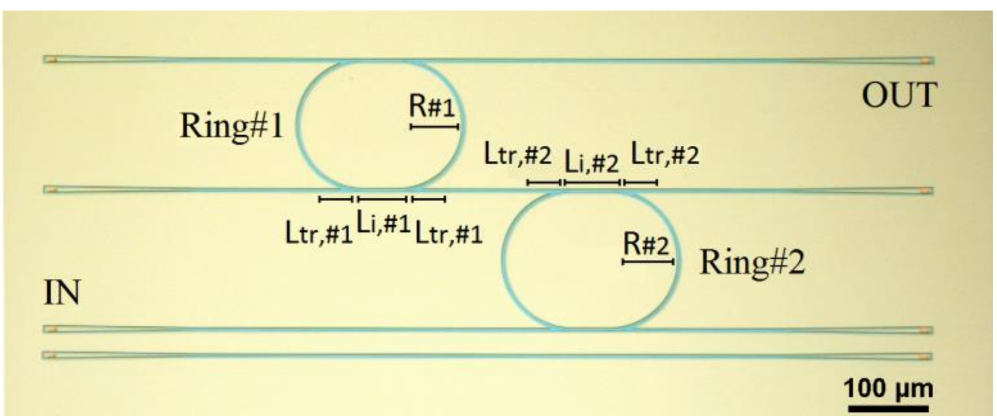

Micrograph of a representative Vernier device.

PHOTONICS RESEARCH GROUP

CASCADE-COUPLED RACETRACK RESONATORS – LONG RACETRACKS

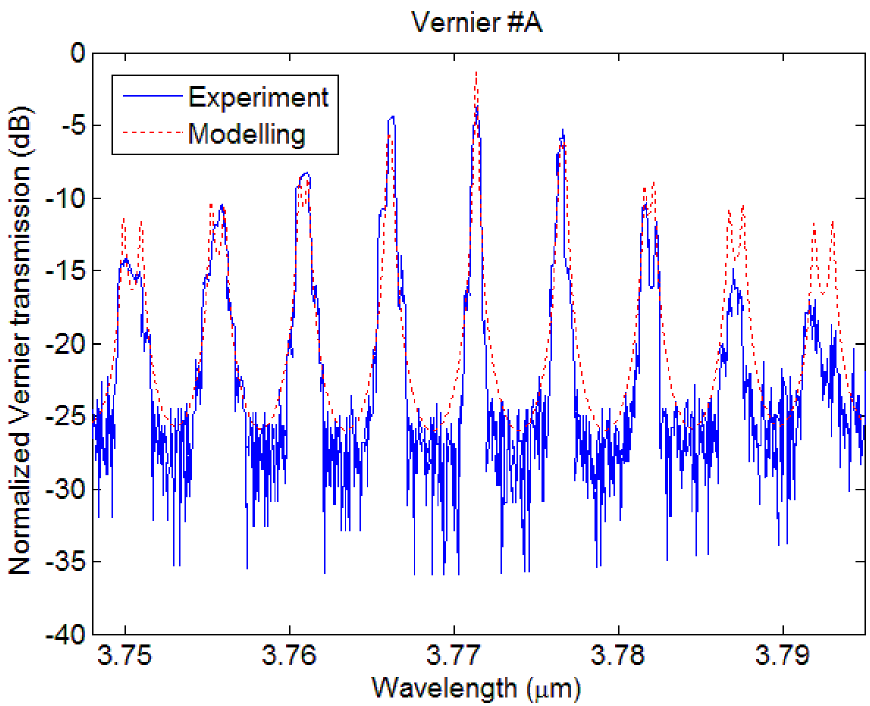

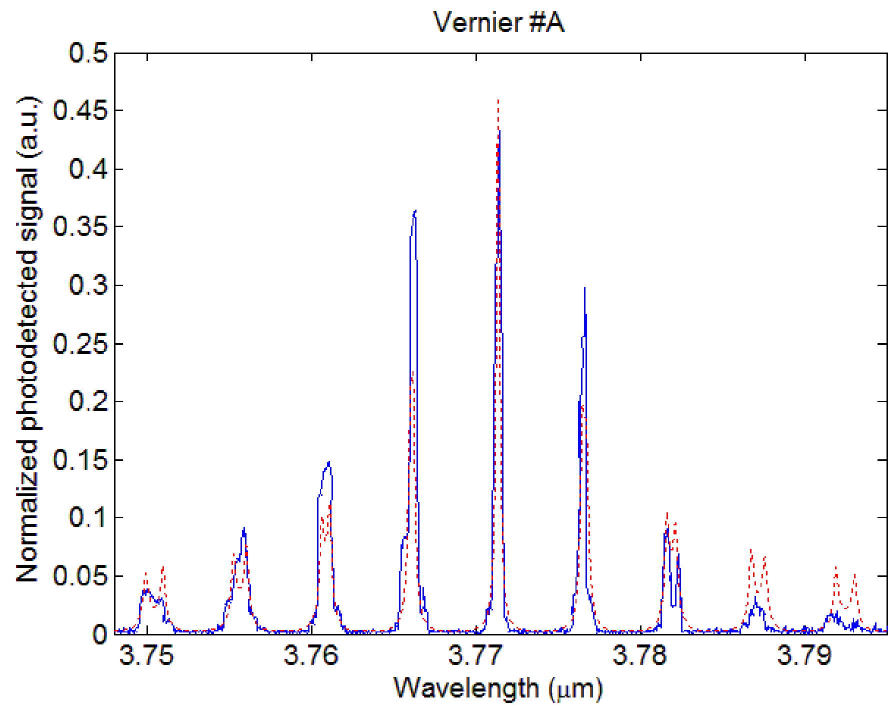

Optical parameters	Vernier #A	Vernier #B
IL (dB)	3.6	< 1
ER (dB)	25	25
Q-factor	8,000	3,200
$\Delta\lambda_{Vernier}$ (nm)	~ 5.5	~ 14
ΔFSR (nm)	0.27	0.74
$FSR_{Vernier}$ (nm)	98	249
G	19.40	18.87

Lengths > 700 μm

<u>SOI rib waveguides</u>

Vernier A: n = 19

mid infrared range

PHOTONICS RESEARCH GROUP

CASCADE-COUPLED RACETRACK RESONATORS – SHORT RACETRACKS

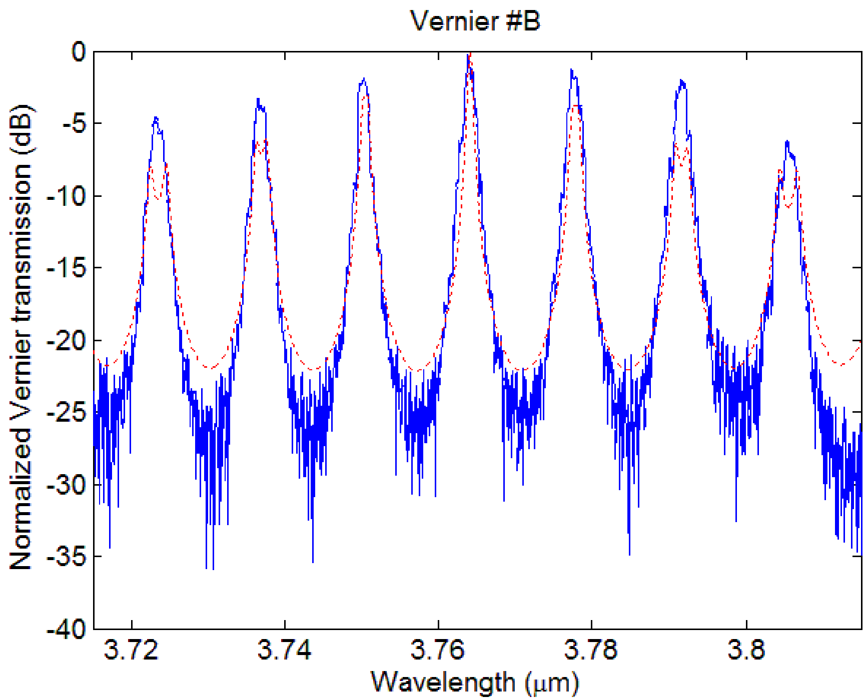

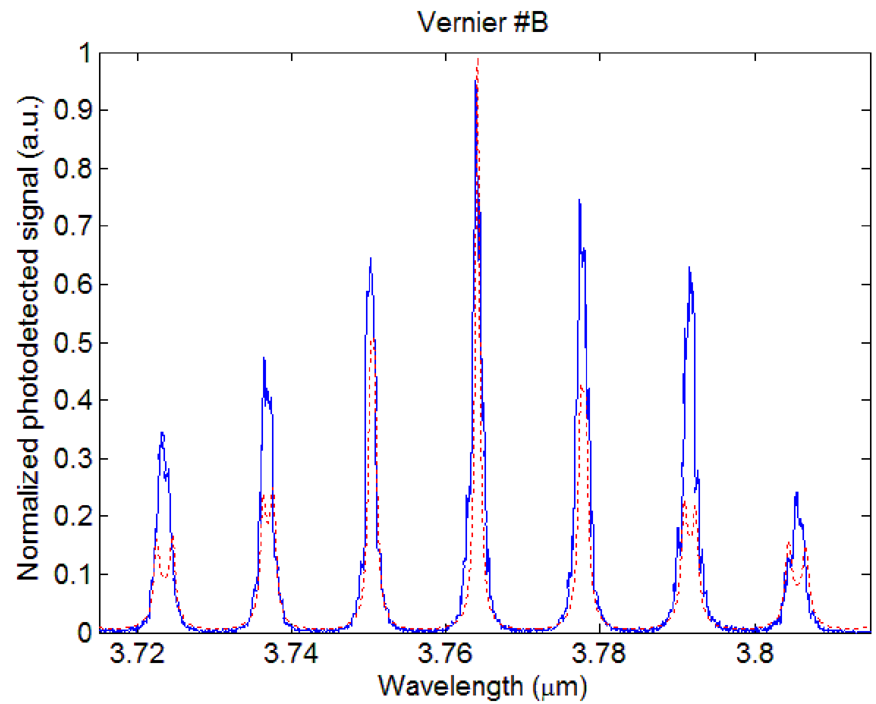

Optical parameters	Vernier #A	Vernier #B
IL (dB)	3.6	< 1
ER (dB)	25	25
Q-factor	8,000	3,200
$\Delta\lambda_{Vernier}$ (nm)	~ 5.5	~ 14
ΔFSR (nm)	0.27	0.74
$FSR_{Vernier}$ (nm)	98	249
G	19.40	18.87

Lengths < 300 μm

SOI rib waveguides

Vernier B: n = 28

mid infrared range

CASCADE-COUPLED RACETRACK RESONATORS

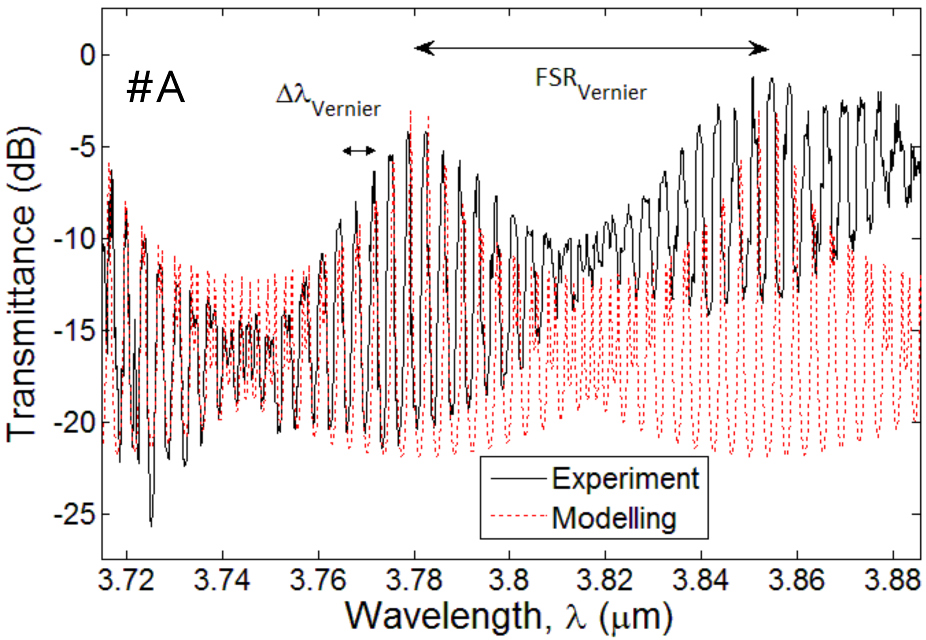

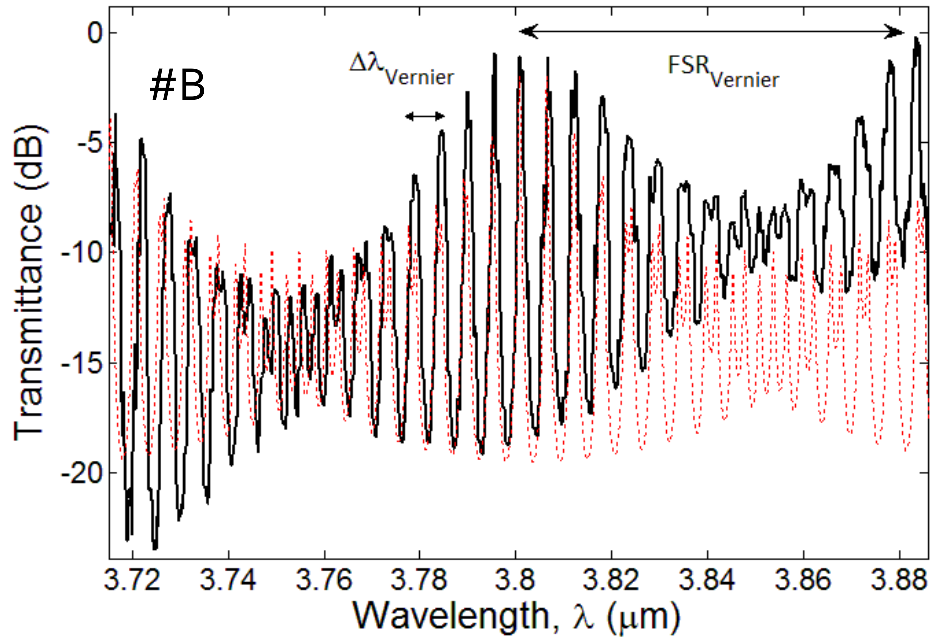

Optical parameters	Vernier #A	Vernier #B
IL (dB)	3.85	2.39
ER (dB)	16.97	18.19
$\Delta\lambda_{Vernier}$ (nm)	~ 4	~ 6
ΔFSR (nm)	0.19	0.32
$FSR_{Vernier}$ (nm)	71.81	99.32
G	19.94	18.12

SOI wire waveguides

mid infrared range

PHOTONICS RESEARCH GROUP

SENSING FUNCTIONALITIES

- PDMS microfluidic channel placed on top of the SOI chip. Perfluorodecalin (a liquid fluorocarbon to dissolve gases), which is low loss at mid-infrared wavelengths, has been used as liquid sample in the sensing chamber.

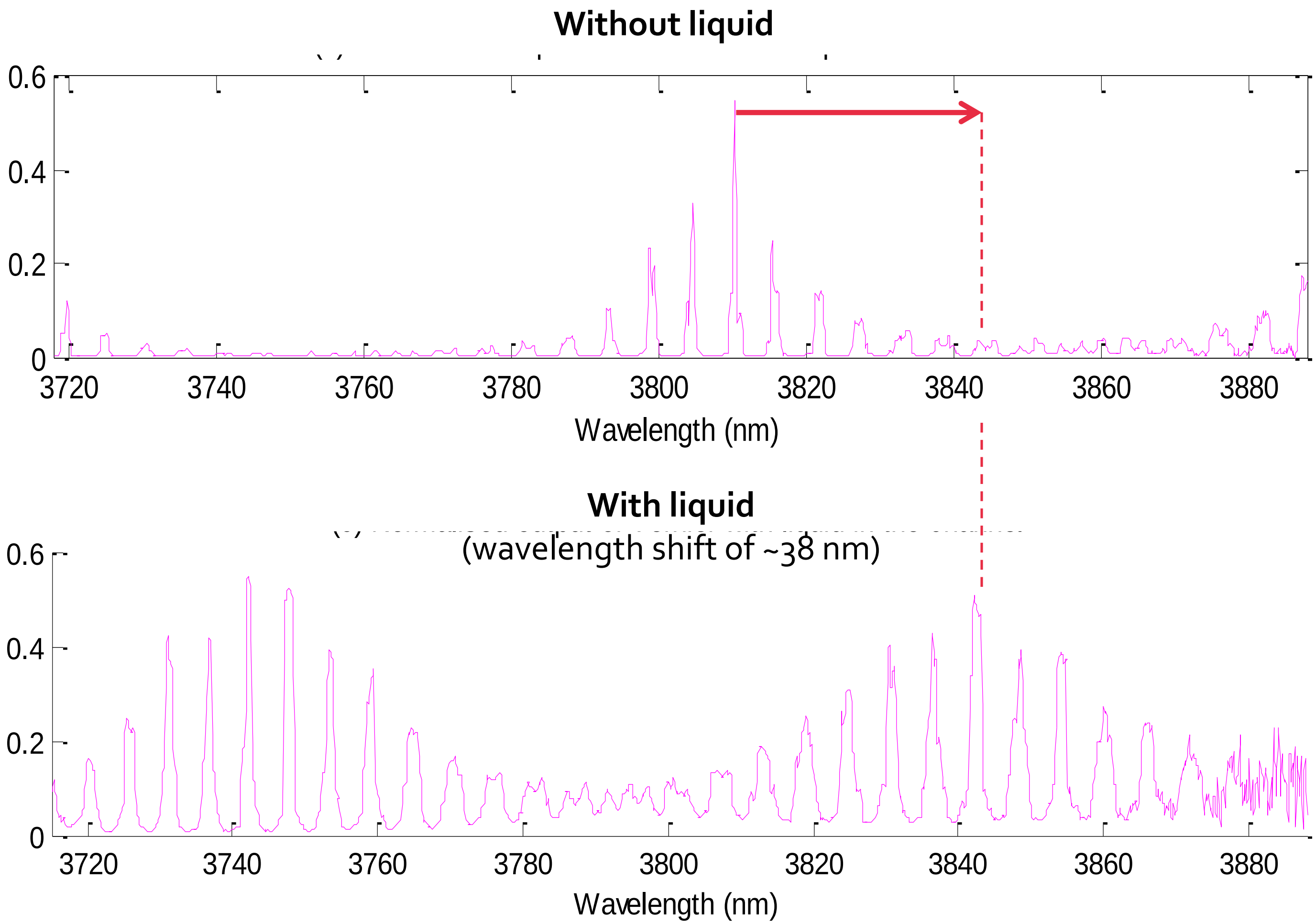

PHOTONICS RESEARCH GROUP

Germanium Vernier-effect ring resonators (for longer wavelengths ~10 micron)

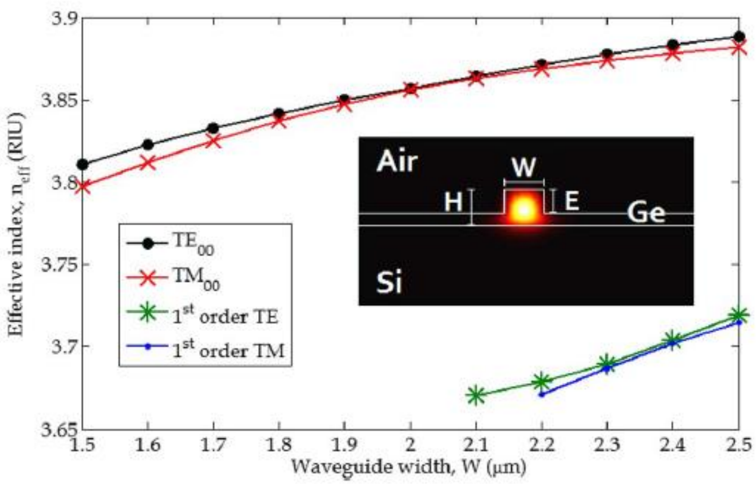

Cross-sectional view of the Ge-on-Si waveguide operating at 3.8 μm.

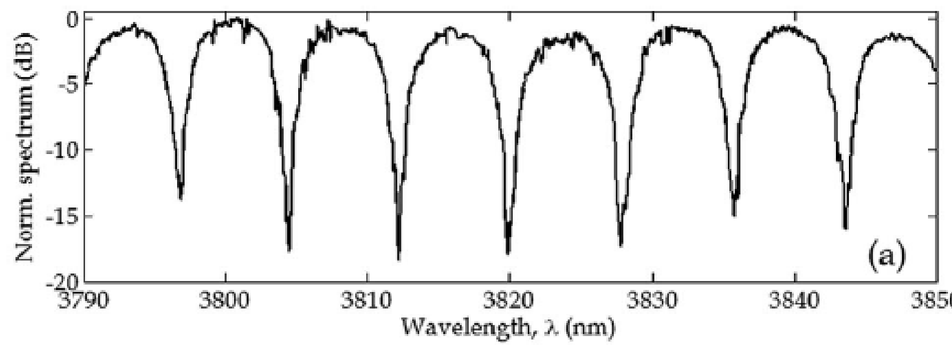

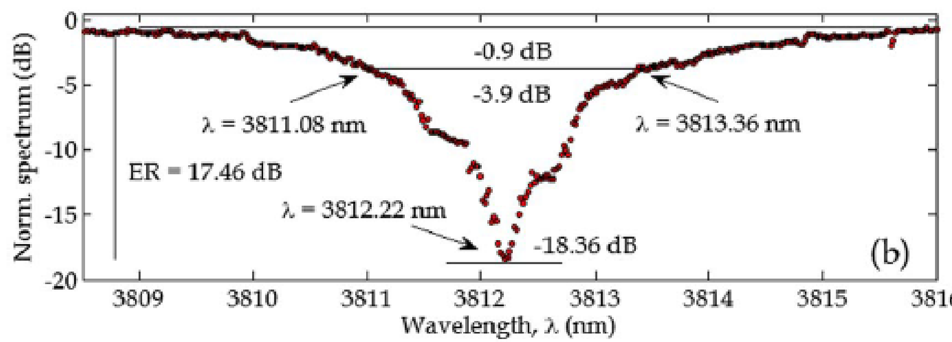

Table 1. Geometrical Parameters of Vernier #A and Vernier #B Architectures

	Vernier #A		Vernier #B	
Parameters	RR #A1	RR #A2	RR #B1	RR #B2
L (μm)	439.60	449.60	1039.30	1079.10
R (μm)	59	59	142	149
L_i (μm)	34.44	39.44	73.54	71.45
g_0 (nm)	450	450	650	650

First experimental demonstration of integrated ring resonator based on Ge-on-Si technology platform operating in the mid-IR. A quality factor of Q ~ 1,700 has been achieved.

$$\frac{FSR''}{FSR'} = \frac{L'}{L''} = \frac{n-1}{n}$$

Vernier A: n = 45, G = 43.4
Vernier B: n = 27, G = 25.4

PHOTONICS RESEARCH GROUP

B. Troia et al., Opt. Lett., Vol. 41, no. 3, pp. 611-613 (2016).

GERMANIUM VERNIER-EFFECT RING RESONATORS

Vernier #B

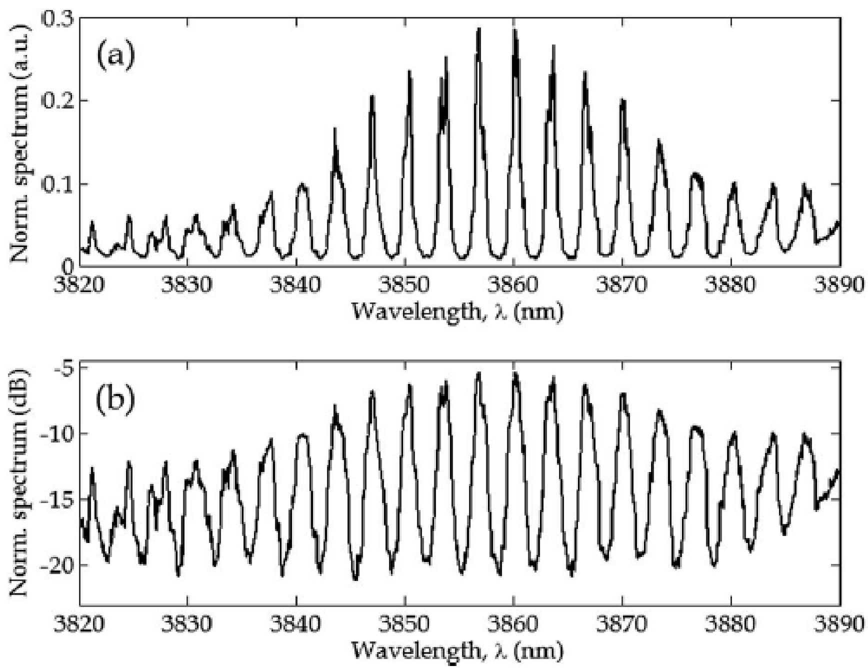

Vernier #A

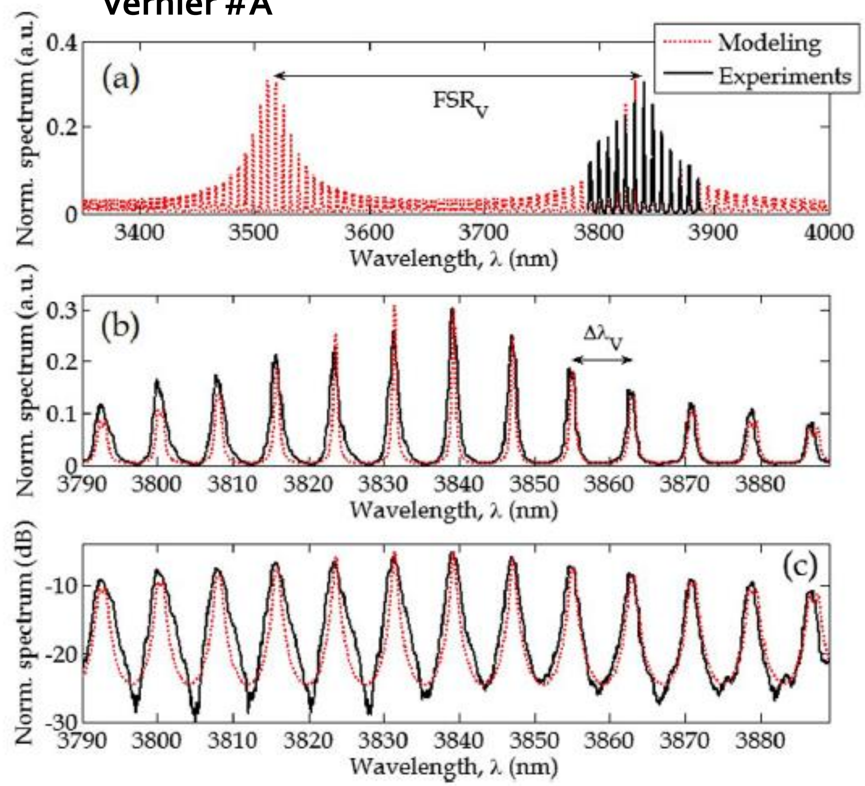

	Vernier #A		Vernier #B	
Parameters	RR #A1	RR #A2	RR #B1	RR #B2
FSR (nm)	7.82	7.64	3.31	3.18
κ_c^2	0.042	0.051	0.068	0.066
IL_V (dB)	5.17		5.42	
ER_V (dB)	20.45		15.00	
Q_V	3147		5361	
$\Delta\lambda_V$ (nm)	~7.50		~3.10	
ΔFSR (nm)	0.18		0.13	
FSR_V (nm)	331.91		80.96	
G_V	43.44		25.46	

Vernier #A and Vernier #B spectra in the mid-IR.
A good agreement between theoretical and experimental spectra can be seen.
The periodicity of the Vernier spectra cannot be measured because of the limited laser wavelength range.

PHOTONICS RESEARCH GROUP

B. Troia et al., Opt. Lett., Vol. 41, no. 3, pp. 611-613 (2016).

EXPERIMENTAL DEMONSTRATION OF RING RESONATOR IN THE NIR-IR

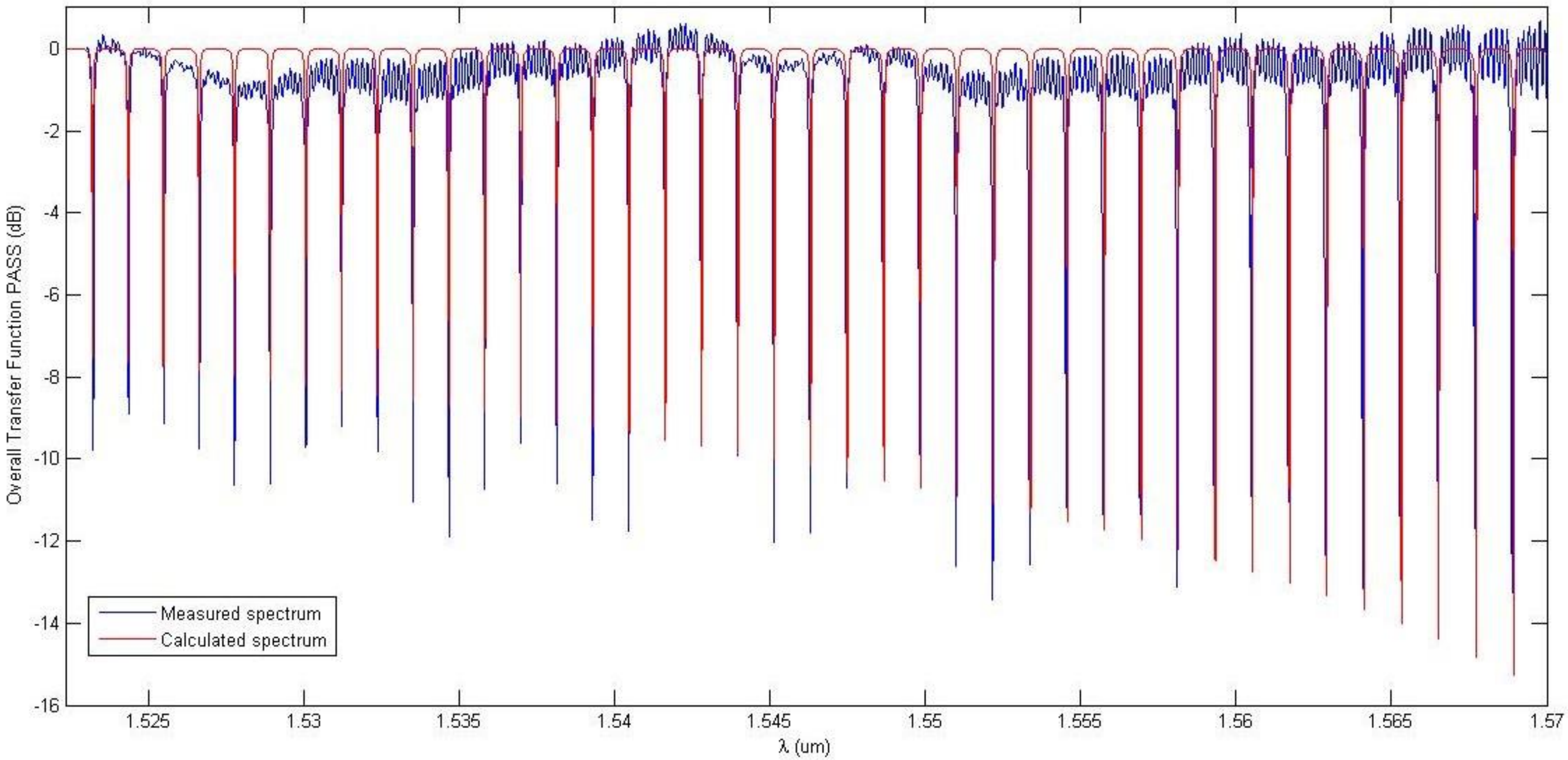

Device dimensions:

- **Ring radius = 77 μm;**
- Overall length = 500.7 μm;
- Directional coupler gap = 500 nm;
- Interaction length = 8.4474 μm.

Extinction ratio is a function of wavelength-dependent coupling coefficient

PHOTONICS RESEARCH GROUP

EXPERIMENTAL DEMONSTRATION OF THE VERNIER EFFECT IN THE NIR-IR

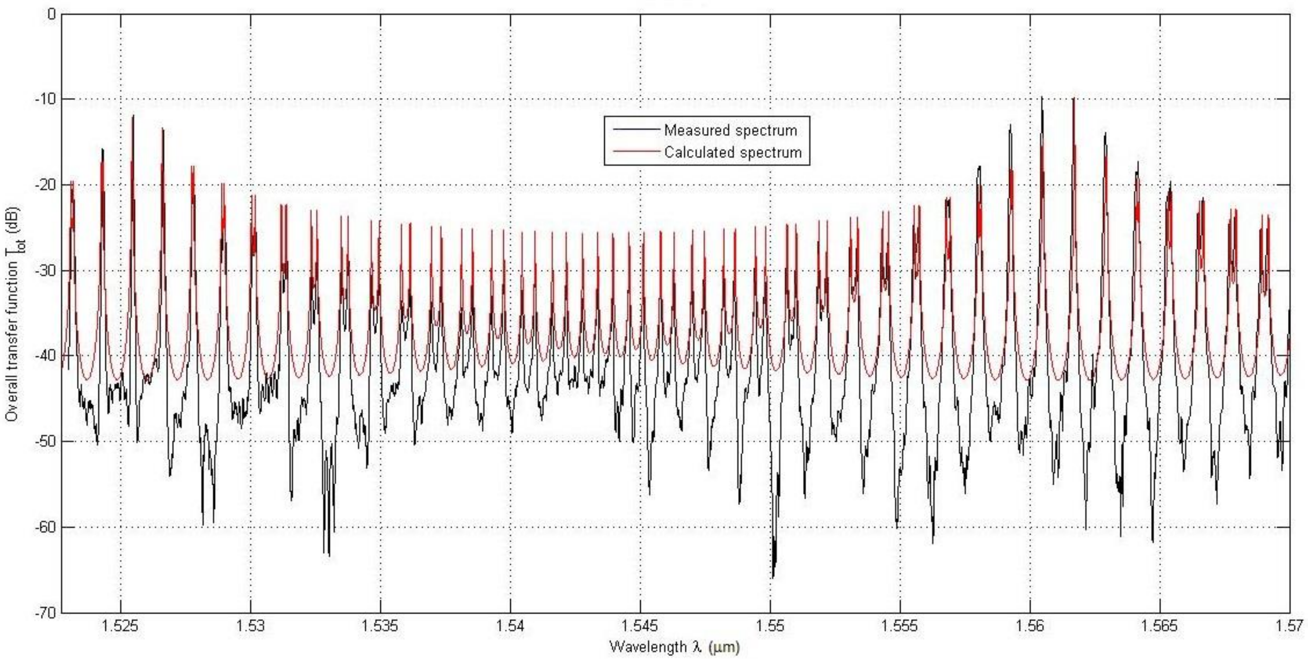

Vernier configuration operating in the second regime: **very good agreement between theory and experiments in near-IR.**

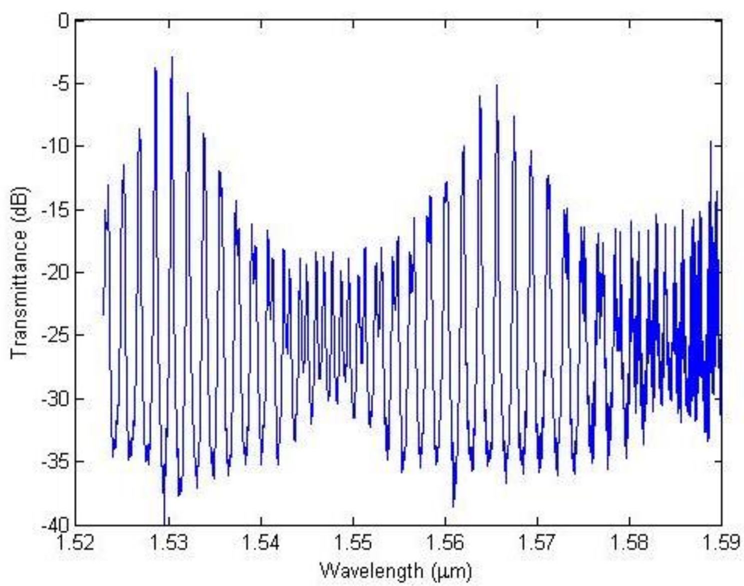

Device dimensions:

Ring radius (filter) = 77 μm
Ring radius (sensor) = 79 μm

Ring radius (filter) = 49 μm
Ring radius (sensor) = 52 μm

PHOTONICS RESEARCH GROUP

EXPERIMENTAL DEMONSTRATION OF THE VERNIER EFFECT IN THE NEAR-IR

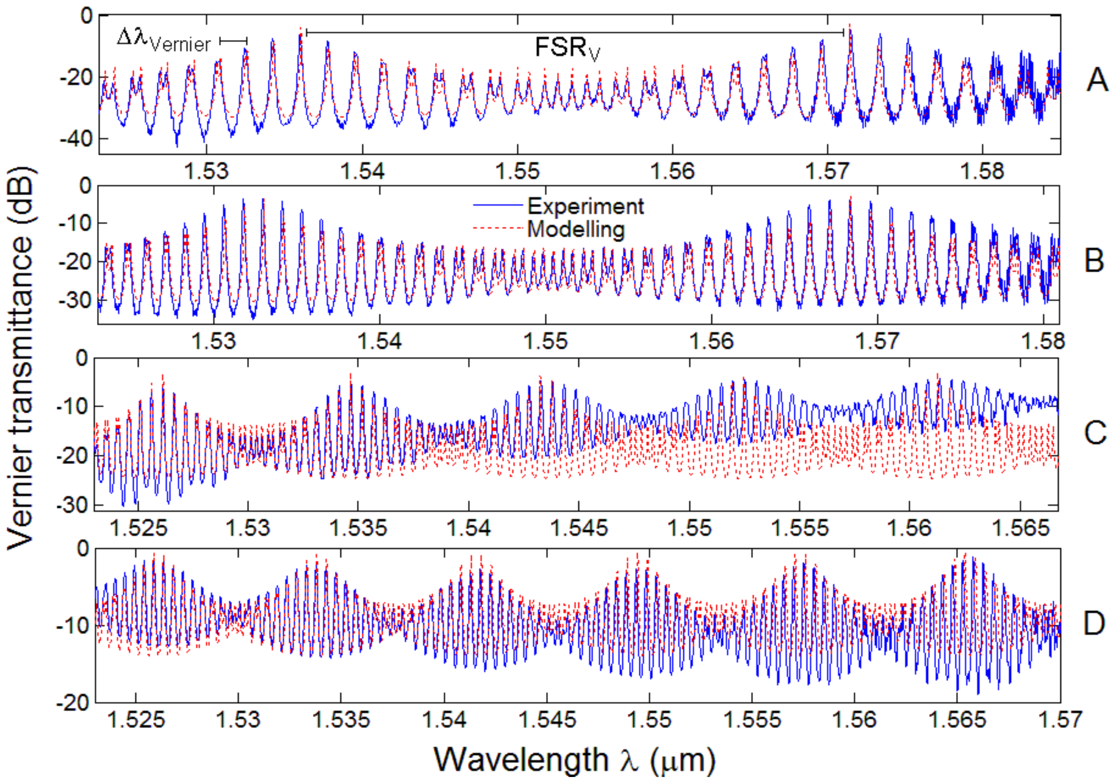

Reducing the Vernier FSR and Vernier gain going from A to D

Device	FSR_v (nm)	$FSR_{v,exp}$ (nm)	ε_{r,FSR_v} %	G	G_{exp}	$\varepsilon_{r,G}$ %
A	35.86	35.50	1.00	20.18	20.20	-0.09
B	35.86	35.61	0.69	30.28	30.30	-0.06
C	9.00	8.89	1.22	17.42	17.30	0.68
D	7.91	7.84	0.88	16.53	16.40	0.78

Vernier configuration operating in the second regime:
very good agreement between theory and experiments.

PHOTONICS RESEARCH GROUP

OUTLINE

- PHOTONIC SENSING APPLICATIONS
- PHOTONIC DEVICES FOR SENSING APPLICATIONS
  - Design of photonic waveguides;
  - Optical sensing principles;
  - Group IV material systems and alloys.
- PHOTONIC ARCHITECTURES BASED ON VERNIER EFFECT
  - The Vernier effect for photonic sensing;
  - Vernier sensors based on cascaded microring resonators;
  - Vernier sensors based on cascaded ring resonator and MZI;
  - Vernier sensors based on cascaded ring resonator and MZI with a Sagnac loop.
- ADVANCED PHOTONIC SENSORS OPERATING IN THE NEAR-IR AND MID-IR
  - Sensing principles for gas detection in the mid-IR;
  - Photonic sensors based on the Vernier effect for methane and ethane detection;
  - Experimental demonstration of the Vernier effect in integrated Photonics.
- **CONCLUSIONS**

CONCLUSIONS

Ultra-high performance photonic sensors based on Vernier effect

- *Real-time* monitoring;
- High-throughput screening;
- Immunity to electromagnetic interferences;
- Intensity and wavelength optical readouts;
- Customizable photonic sensor designed as a function of the sensing application.

Vernier configuration based on ring resonators for biochemical sensing in near-IR.

Performance	***m-xilene* detection**	**Pb(II) detection in water**
Sensitivity	149.74 µm/RIU	182.36 µm/RIU
Resolution	< 60 ppm	< 50 ppb
Limit of detection (LOD)	4.0403×10^{-6} RIU	3.5373×10^{-6} RIU

Silicon-on-insulator (SOI) and *Germanium-on-Silicon* CMOS-compatible technologies

- CMOS-compatible;
- Small footprint (~mm^2);
- Large scale production;
- Low cost;
- *Lab-on-chip* (state-of-the-art).

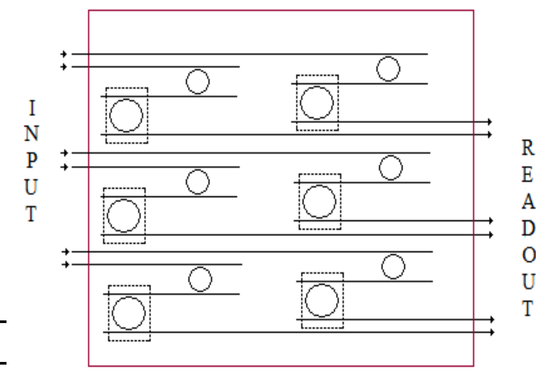

Sensor matrix

Performance @ 3.39 µm	***methane***	***ethane***
Sensitivity	224.4 µm/RIU	218.51 µm/RIU
Resolution [% in air volume]	~ 2 %	~ 1 %
Limit of detection (LOD)	1.9568×10^{-5} RIU	2×10^{-5} RIU

Vernier architecture based on ring resonators for gas sensing in mid-IR.

PHOTONICS RESEARCH GROUP

RELEVANT PUBLICATIONS ON THE TOPIC

Some papers on integrated photonic sensors and Vernier effect devices

- V.M.N. Passaro, M. La Notte, "Optimizing SOI Slot Waveguide Fabrication Tolerances and Strip-Slot Coupling for Very Efficient Optical Sensing", Sensors, vol. 12, n. 3, pp. 2436-2455, 2012.
- V.M.N. Passaro, B. Troia, F. De Leonardis, "A generalized approach for design of photonic gas sensors based on Vernier effect in mid-IR", Sensors and Actuators B: Chemical, vol. 168, pp. 402-420, 2012.
- V.M.N. Passaro, B. Troia, M. La Notte, F. De Leonardis, "Photonic resonant microcavities for chemical and biochemical sensing", RSC Advances, vol. 3, pp. 25-44, 2013 (INVITED).
- M. La Notte, V.M.N. Passaro, "Ultra high sensitivity chemical photonic sensing by Mach-Zehnder interferometer enhanced Vernier-effect", Sensors and Actuators B: Chemical, vol. 176, pp. 994-1007, 2013.
- B. Troia, F. De Leonardis, V.M.N. Passaro, "Generalized modelling for the design of guided-wave optical directional couplers," Optics Letters, Vol. 39, No. 5, pp. 1161-1164, 2014.
- B. Troia, and V. M. N. Passaro, "Investigation of a novel silicon-on-insulator Rib-Slot photonic sensor based on the Vernier effect and operating at 3.8 µm," J. Europ. Opt. Soc. Rap. Public., vol. 9, pp. 14005-1 – 14005-6, 2014.
- M. La Notte, B. Troia, T. Muciaccia, C. E. Campanella, F. De Leonardis, and V. M. N. Passaro, "Recent Advances in gas and Chemical Detection by Vernier Effect-based Photonic Sensors," Sensors, vol. 14, n. 3, pp. 4831-4855, 2014.
- B. Troia, Ali Z. Khokhar, M. Nedeljkovic, J. S. Penades, V.M.N. Passaro, G.Z. Mashanovich, "Cascade-coupled racetrack resonators based on the Vernier effect in the mid-infrared", Optics Express, vol. **22**, n. 20, pp. 23990-24003, 2014.
- R. Bruck, B. Mills, B. Troia, D.J. Thomson, F.Y. Gardes, Y. Hu, G.Z. Mashanovich, V.M.N. Passaro, G.T. Reed, O.L. Muskens, "Device-level characterization of the flow of light in integrated photonic circuits using ultrafast photomodulation spectroscopy," Nature Photonics, vol. **9**, n. 1, pp. 54-60, 2015. doi: 10.1038/NPHOTON.2014.274, published online on 17 Nov 2014.
- B. Troia, A.Z. Khokhar, M. Nedeljkovic, S.A. Reynolds, Y. Hu, G.Z. Mashanovich, V.M.N. Passaro, "Design Procedure and Fabrication of Reproducible Silicon Vernier Devices for High Performance Refractive Index Sensing," Sensors, vol. **15**, pp. 13548-13567, 2015.
- B. Troia, M. Nedeljkovic, A. Khokhar, J. Soler Penades, C. Alonso Ramos, V.M.N. Passaro, G.Z. Mashanovich, "Germanium-on-silicon Vernier-effect photonic microcavities for the mid-infrared," Optics Letters, vol. **41**, n. 3, pp. 610-613, 2016.
- B. Troia, F. De Leonardis, V.M.N. Passaro, "Cascaded ring resonator and Mach-Zehnder interferometer with a Sagnac loop for Vernier-effect refractive index sensing," Sensors and Actuators B: Chemical, vol. **240**, pp. 76-89, 2017.
- B. Troia, J. S. Penades, Z. Qu, A. Z. Khokhar, A. Osman, Y. Wu, C. Stirling, M. Nedeljkovic, V.M.N. Passaro, G. Z. Mashanovich, "Silicon ring resonator-coupled Mach-Zehnder interferometers for the Fano resonance in the mid-IR," Applied Optics, vol. **56**, n. 31, pp. 8769-8776, 2017.

PHOTONICS RESEARCH GROUP